Fig. 1. Computed tomography of the brain showing bilateral atrophy of the frontal and temporal lobes with pallidal calcification (Case 8).

FTLD-U and amyotrophic lateral sclerosis (ALS) [8,9]. Subsequent studies have demonstrated the concurrence of TDP-43, tau, and alpha-synuclein (aSyn) pathology in other neurodegenerative disorders including AD, Dementia with Lewy bodies (DLB), Guamanian ALS/parkinsonism–dementia complex (G-PDC) and argyrophilic grain disease (AGD) [10–14]. However, it remains unclear whether or not these pathological proteins coexisted within the same neuron. In addition, although the clinical symptoms of DNTC have been attributed to a partial mixture of AD and FTLD [1], the way in which these neuropathological changes contribute to the clinical symptoms is not fully understood at present. Especially because the symptoms of DNTC clinically closely mimic those of FTLD, it is important to observe the pathology of DNTC specifically for a comparison with FTLD.

In order to clarify the proteinopathy of DNTC in this study, 1) we performed detailed immunohistochemical analyses of 10 Japanese DNTC cases, using phosphorylation-dependent anti-TDP-43 antibodies and anti aSyn antibodies. 2) Furthermore, we investigated the colocalization or non-colocalization of these proteins in DNTC using the technique of double-label immunofluorescence staining. 3) In addition, we considered the correlation between the clinical symptoms and the neuropathological findings based on the immunohistochemical investigations mentioned.

2. Materials and methods

2.1. Materials

Ten autopsied DNTC cases were examined (2 male, 8 female). The age at death ranged from 56 to 79 years (average 67.0 years). The weights of the brains ranged from 850 to 1265 g (average 1050 g) (Table 1). In all cases except one (Case 9), there were temporal or frontotemporal lobar atrophy, widespread NFTs, a paucity of plaques and pronounced Fahr's-type calcification in the basal nuclei or cerebellum, consistent with the neuropathological criteria of DNTC [2]. Case 9 was previously diagnosed as DNTC despite a lack of atrophy [15]. Detailed clinical data on some cases were previously reported elsewhere [1,16].

2.2. Methods

2.2.1. Tissue preparations

The brains were fixed with 10% buffered formalin and paraffin-embedded. Brain blocks of the frontal lobe, parietal lobe, temporal lobe, brainstem, and limbic region (including the amygdala, retro hippocampal formation, and parahippocampal gyrus), were cut into 5 μm-thick slices in the coronal section. All sections were stained with hematoxylin and eosin, Klüver–Barrera's method and Gallyas–Braak method (GB).

2.2.2. Immunohistochemistry

Immunohistochemistry was carried out using the avidin–biotin peroxidase complex technique (Vectastain ABC Kit; Vector Laboratories, Burlingame, CA, USA). Immunohistochemical staining was performed using anti-phosphorylated aSyn (Wako, concentration 1:3000), anti-TDP-43 (Protein Tech, 1:2000), and anti-phosphorylated TDP-43 (pTDP) (pS409/410 and pS403/404 [17], 1:1000, respectively). Some specimens were stained with anti-paired helical filament tau mouse monoclonal antibody (AT8; Innogenetics, Zwijndrecht, Belgium, 1:100). The sections were finally mounted in a glycerol-based medium and then observed using a light microscope. The Lewy body type, and the degree and distribution of Lewy pathology, were assessed by pathologic assessment and diagnostic criteria for DLB [18]. Furthermore, we assessed the TDP-43 pathology following the study of Amador-Ortiz, C. et al. [10]. Cases having more severe pathology outside of the temporal lobe were considered to have "diffuse" TDP-43 immunoreactivity. Cases with involvement relatively confined to the limbic lobe were referred to as "limbic." The TDP-43-positive structure was assessed using the following scheme: 0 = none, 1 = slight, 2 = mild, 3 = moderate, 4 = severe.

2.2.3. Double labeling immunofluorescence study

A double labeling immunofluorescence study was performed for pTDP-43 and phosphorylated tau, or for pTDP-43 and phosphorylated aSyn in Cases 2 and 8. The sections were incubated overnight at 4 °C in a cocktail of pS403/404 [17] and AT8 (Innogenetics, 1:100) or anti aSyn (Wako, 1:3000). After washing with PBS containing 0.3% Triton X-100 (Tx-PBS) for 30 min, the sections were incubated for 2 h at room temperature in a cocktail of fluorescein isothiocyanate-conjugated goat anti-mouse IgG (1:100; Millipore, Temecula, CA) and tetramethylrhodamine isothiocyanate-conjugated goat anti-rabbit IgG (1:100; Millipore). After washing, the sections were incubated in 0.1% Sudan Black B for 10 min at room temperature and washed with Tx-PBS for 30 min. The sections were coverslipped with Vectashield (Vector Laboratories) and observed with a confocal laser microscope (LSM5 PASCAL; Carl Zeiss MicroImaging GmbH, Jena, Germany).

2.2.4. Relationship between histopathology and clinical features

The clinically characteristic symptoms were investigated and summarized from the clinical charts and previous reports [1,15,16]. From this information, we assessed the neuropsychiatric symptoms of the 10 cases referring to the evaluation items of the Neuropsychiatric Inventory Questionnaire (NPI-Q) [19], in addition to cognitive and functional decline and verbal disturbance. We extracted three items from NPI-Q which are supposed to be marked, especially in FTLD cases: a) apathy or indifference, b) disinhibition (impulsiveness), and c) motor disturbance (pacing, compulsive behaviors). We investigated the statistical relationships between the scores of these characteristic items and the severity score of pathological findings. Statistical analyses were performed using Spearman's correlation coefficient method with $p<0.05$ considered statistically significant.

Table 1
Clinical features and neuropathological findings of 10 DNTC cases.

Case					1	2	3	4	5	6	7	8	9	10
Clinical diagnosis					PSD	AD	PSD	PiD	NANPD	AD+BD	NANPD	PiD	SPs	Sc
General information	Background	Sex			F	F	F	M	F	F	M	F	F	F
		Age at onset (years old)			46	49	51	52	56	56	59	64	65	NA
		Age at death (Duration years)			68(22)	57(8)	59(8)	56(4)	64(8)	79(17)	73(4)	72(8)	70(5)	72
		Cause of death			Pn	Inf	Inf	Pn	Pn	Inf	RnF	RnF	Pn	RnF
		Heredity			No	No	No	No	No	CVD, Sc	No	No	No	No
		Past history			No	No	Tb	No	No	Con	No	Men	No	SAH
	Brain	Weight (g)			850	1050	1140	1260	1000	920	1030	970	1265	1015
		Atrophy region			FL, TL	FL, TL	TL	FL, TL	TL	FL,TL	FL, TL	FL, TL	None	TL
Clinical findings	Memory disturbances (None, ±, +, ++)				++	+	+	±	+	+	+	+	±	None
	Verbal disturbances (None, +)				None	+	+	+	+	+	+	+	+	None
	Neurological symptoms				Pa, Ps	None	None	Pa	None	Dev	Pa, Ps	None	None	None
	†Personality changes	Three extracted items of NPI-Q score	Apathy		12	8	12	12	2	0	8	0	8	12
			Disinhibition		12	12	0	0	0	0	12	12	12	0
			Motor disturbance		0	0	12	8	0	0	12	8	0	8
			Total score		24	20	24	20	2	0	32	20	20	20
Pathological findings	††TDP-43 pathology	Distribution pattern			Limbic	Diffuse	Diffuse	Diffuse	Diffuse	Limbic	Diffuse	Diffuse	NA	Diffuse
		†††FTLD-TDP subtype			NA	2	2	2	2	NA	3	2	NA	2
		TDP-43 score	PC		0	1	0	0	0	0	3	0	0	1
			FC and TC	FC	NA	0	0	0	0	0	0	NA	0	0
				TC	0	2	1	3	2	0	4	2	0	4
				Total score	0	2	1	3	2	0	4	2	0	4
			LR	AMYG	4	NA	1	1	1	1	4	1	0	2
				HIP	1	2	1	0	0	1	1	2	0	1
				DG	0	1	0	0	0	0	0	0	0	0
				EC	0	3	1	3	1	0	2	2	0	2
				Total score	5	6	3	4	2	2	7	5	0	5
			FC, TC and LR total score		5	8	4	7	4	2	11	7	0	9
			BN		0	0	0	0	1	0	0	0	0	1
			Brain stem	SN	NA	NA	1	NA	1	NA	1	1	NA	1
	††††Lewy pathology	Distribution pattern			Limbic	NA	Limbic	Diffuse neocortical	Limbic	Diffuse neocortical	Diffuse neocortical	Diffuse neocortical	NA	Diffuse neocortical
		aSyn score	LR	HIP	2	0	3	4	3	4	4	4	0	4
				DG	0	0	0	1	0	3	1	0	0	0
			Brain stem	SN	NA	NA	2	NA	2	NA	3	2	NA	2
	Tau pathology	NFT (Braak Stage)			VI	VI	VI	VI	VI	VI	VI	VI	VI	VI

AD: Alzheimer's disease, AMYG: amygdala, aSyn: alpha-synuclein, BD: Binswanger's Disease, BN: basal nuclei, Con: convulsion, CVD: cerebrovascular disease, Dev: tongue deviation on protrusion, DG: hippocampal dentate gyrus, EC: entorhinal cortex, F: female, FC: frontal cortex, FL: frontal lobe, HIP: hippocampus, Inf: infection, LR: limbic region, M: male, Men: meningitis, NA: not available, NANPD: non-Alzheimer non-Pick dementia, NFT: neurofibrillary tangles, NPI-Q: Neuropsychiatric Inventory Questionnaire, Pa: parkinsonism, PC: parietal cortex, PiD: Pick disease, Pn: pneumonia, Ps: pyramidal sign, PSD: presenile dementia, RnF: renal failure, SAH: subdural hemorrhage, Sc: schizophrenia, SN: substantia nigra, SPs: senile psychosis, Tb: pulmonary tuberculosis, TC: temporal cortex, TDP-43: TDP-43: TAR DNA-binding protein of 43 kDa, TL: temporal lobe.

†Personality changes were assessed according to the Neuropsychiatric Inventory Questionnaire (score 0–12).

††The distribution pattern of TDP-43 was assessed following the study of Amador-Ortiz et al. [10]. The TDP-43-positive inclusions were assessed using the following scheme: 0: none, 1: slight, 2: mild, 3: moderate, and 4: severe.

†††FTLD-TDP subtype was assessed using the classification of Sampathu et al. [24].

††††The Lewy body type, and the degree (alpha-synuclein score (0–4)) and distribution of Lewy pathology, were assessed by pathologic assessment and diagnostic criteria for DLB (McKeith et al. [18]).

Statistical analyses were performed using Spearman's correlation coefficient method with $p<0.05$ considered statistically significant.

* $p>0.05$, ** $p<0.05$, *** $p>0.05$.

3. Results

3.1. Pathological findings

3.1.1. Tau pathology

In all cases, GB stain showed widespread and abundant NFTs throughout the neocortex and limbic system, especially the temporal cortex, hippocampus, and amygdala. The distribution pattern of NFTs indicated that all cases were classified as stages V or VI based on Braak and Braak staging [20].

3.1.2. The aSyn pathology

Alpha-Syn positive inclusions and neurites were observed in 8 cases (Cases 1, 3, 4, 5, 6, 7, 8, 10 in Table 1). The distribution of aSyn pathology was confined to the limbic region in 3 (Cases 1, 3, 5) of 8 cases, and extended to the neocortex in the other 5 cases. The former 3 cases were identified as the limbic type, and the latter 5 cases as the diffuse neocortical type, according to the classification of DLB by the study of McKeith et al. [18] (Table 1) (Fig. 2A). In the limbic region, aSyn-positive structures were present in dentate granule cells of the hippocampus in 3 cases (Cases 4, 6, 7) (Fig. 2B), in pyramidal neurons of CA2 and CA3 areas in 6 cases (Cases 3, 4, 6, 7, 8, 10) (Fig. 2C), and in the deep layer of the parahippocampal cortex in all 8 cases (Fig. 2D–F).

3.1.3. TDP-43 pathology

The pTDP-43 immunopositive structures were observed in 9 of 10 cases (Table 1). Regarding the distribution of pTDP-43 pathology, 2

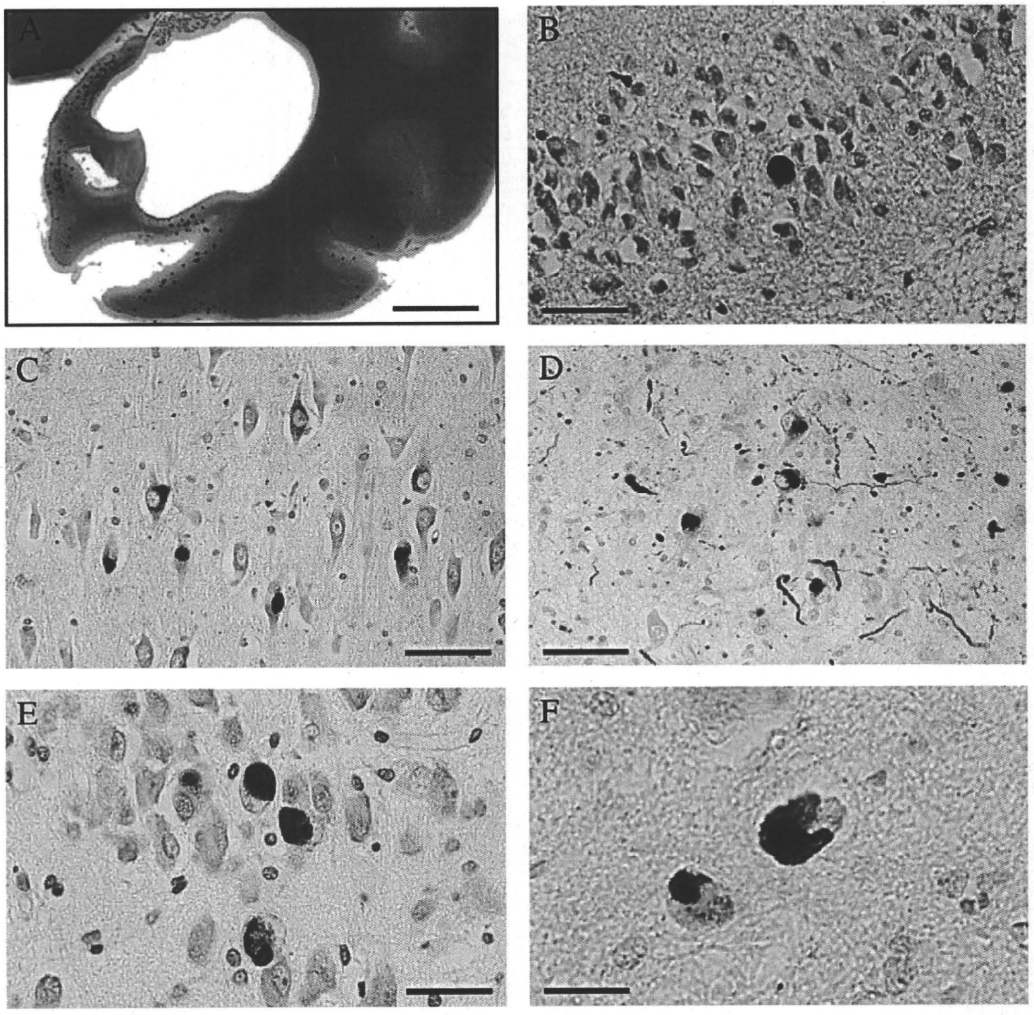

Fig. 2. A. Appearance of Lewy bodies and Lewy neurites in Case 8 (alpha-synuclein immunostaining: one dot indicates one Lewy body). B. Lewy bodies were observed in the dentate granule cell layer in the hippocampus (Case 6). C. Lewy bodies and neurites were observed in CA3 of Case 4. Scale bar = 50 μm. Lewy bodies were observed in the deep layer of the parahippocampal cortex (D (Case 7), E (Case 3), and F (Case 5)). Scale bar: A, 5 mm; B, C, 50 μm; D, E, and F, 20 μm.

of 9 cases showed pTDP-43 pathology confined to the limbic region, while the other 7 cases showed more widespread pTDP-43 pathology to the temporal neocortex. Of the 7 cases with pTDP-43 pathology in the neocortex, 6 cases (Cases 2, 3, 4, 5, 8, 10) showed predominant neuronal cytoplasmic inclusions (NCIs) with a few dystrophic neurites (DNs) (Fig. 3A–D), while Case 7 showed abundant NCIs and DNs (Fig. 3H–J). Glial cytoplasmic inclusions (GCIs) were also observed in all 9 cases (Fig. 3 E–G). NCIs in the dentate granular cells were found only in one (Case 2) of 9 cases. No neuronal intranuclear inclusions were seen in any of the cases.

Neuronal cytoplasmic granular structures positive for pTDP-43 but negative for a commercial anti-TDP-43 antibody were observed in 6 cases (Cases 2, 4, 5, 7, 8, 10) (Fig. 3K, L). Four (Cases 2, 7, 8, 10) of these showed both pTDP-43 positive cytoplasmic granules and NCIs/GCIs, while 2 cases (Cases 4, 5) showed only granules.

3.1.4. Colocalization of TDP-43 and aSyn or Tau

In double labeling immunofluorescence of the sections of the hippocampal region, a scarce colocalization of pTDP-43 and phosphorylated aSyn or a scarce colocalization of pTDP-43 and phosphorylated tau was observed in neuronal cytoplasm with very low frequency. However, we did see partial colocalization of aSyn and pTDP-43 in some neuronal cytoplasmic inclusions in the deep layer of the entorhinal cortex, and partial colocalization of tau and pTDP-43 in some neuronal cytoplasmic inclusions and the dentate gyrus of the hippocampus. Upon double-immunofluorescent labeling of cytoplasmic inclusions, pTDP-43 was scarcely superimposed with aSyn or tau (Fig. 4).

3.2. Clinical features

The clinical features of each patient are summarized in Table 1. Basically, the main symptoms comprised memory disturbances, verbal disturbances, or personality and behavioral changes in all cases. The degree of memory disturbance was moderate to severe in 7 cases (Cases 1, 2, 3, 5, 6, 7, 8). Verbal disturbances were found in 8 cases. Of these, 3 cases (Cases 5, 7, 8) showed verbal symptoms similar to primary progressive non-fluent aphasia, while one case (Case 2) showed semantic dementia-like symptoms. Regarding neurological symptoms, pyramidal signs including Babinski's sign were observed in 2 cases (Cases 1, 7), and parkinsonism in 3 cases (Cases 1, 4, 7).

Neuropsychiatric symptoms, including personality and behavioral changes, were assessed according to NPI-Q. Regarding personality changes, the symptoms of apathy or indifference were severe in 4 cases (Cases 1, 3, 4, 10). The symptoms of disinhibition characterized by morbid impulsion and 'going my way' behavior (i.e., lack of consideration for the feelings of others) were severe in 5 cases (Cases 1, 2,

7, 8, 9). The symptoms of motor disturbances, including pacing and compulsive behavior, were severe in 2 cases (Cases 3, 7).

3.3. Clinical features and pathology

We examined the relationship between the clinical features and aSyn pathology or TDP-43 pathology. Three cases (Cases 4, 6, 7) showed a higher aSyn score with aSyn-positive inclusions in dentate granular cells in the hippocampus and were identified as the diffuse neocortical type. Such cases tended to have neurological symptoms, including rigidity and akinesia (Cases 4, 7 in Table 1).

Two cases with spontaneous features of parkinsonism and progressive cognitive decline (Cases 4, 7, in Table 1) satisfied the clinical diagnostic criteria of possible DLB [18], and were thought to be categorized as the diffuse neocortical type. Among five cases (Cases 3, 5, 7, 8, 10) with brainstem synuclein pathology, only one case (Case 7) clinically showed parkinsonism.

From the viewpoint of clinical characteristics and TDP-43 pathology, cases with frequent pTDP-43-positive NCIs/GCIs in the hippocampus and amygdala tended to show higher scores of certain items in the NPI-Q (Cases 1, 7 in Table 1).

There were no significant correlations between the score of limbic TDP pathology and the score of each extracted item (apathy, disinhibition, and motor disturbances) of NPI-Q focused on three main clinical feature-associated frontotemporal symptoms (Spearman's correlation coefficient; 0.190, 0.459, and 0.394, respectively, all with p-value>0.05). However, there was a significant correlation between the score of limbic TDP pathology and the combined score of these three extracted items (Spearman's correlation coefficient 0.573, p-value<0.05). In contrast, there was no correlation between the sum of the scores of those three extracted items of NPI-Q and the severity score of frontotemporal TDP pathology (Spearman's correlation coefficient 0.200, p-value>0.05), nor the severity score of frontotemporal and limbic total TDP pathology (Spearman's correlation coefficient 0.441, p-value>0.05).

4. Discussion

In this study, we found high frequencies of cerebral accumulation of TDP-43 (90%) and of aSyn (80%) in DNTC. The accumulation of both abnormal proteins was observed in the limbic region most frequently. The immunoreactivity of TDP-43 was observed to further extend to the neocortex, in almost all cases presenting TDP-43 pathology. In addition, a significant correlation between the sum of the scores of certain question items of the NPI-Q and the score of the limbic TDP-43 pathology suggests that the abnormality of TDP-43 plays an important role in the pathological process and FTLD-like symptoms of DNTC.

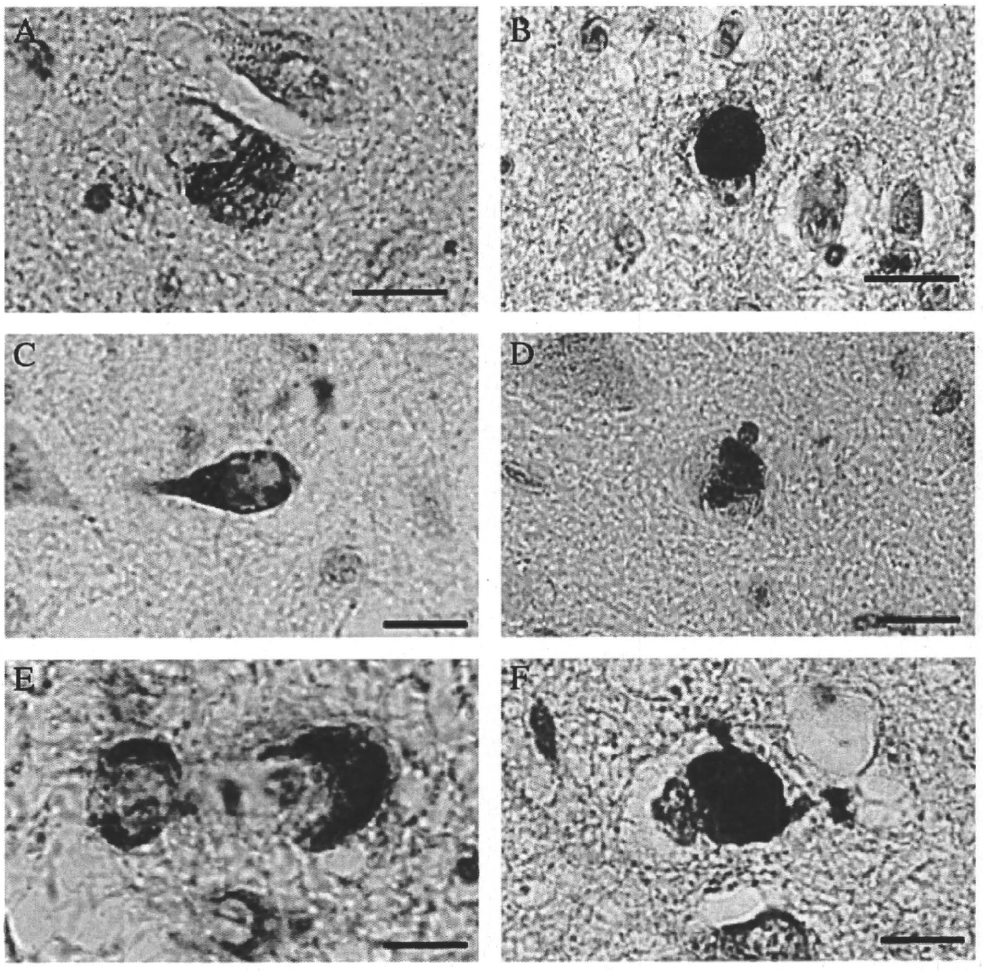

Fig. 3. NCIs were seen in the CA2 areas of Case 8 (A) and Case 1 (B) (anti-pTDP-43). NCIs were seen in the CA2 areas of Case 7 (C) and Case 8 (D) (anti-TDP-43). E. GCI-like structures were observed in the deep layer of the parahippocampal cortex in Case 7 (anti-pTDP). GCI was seen in the CA2 area (F) and CA3 area (G) of Case 2 (anti-pTDP). GCI-like structures and DNs were observed in the deep layer of the middle temporal gyrus (H), in the amygdala (I), and in the deep layer of the parahippocampal cortex (J) of Case 7 (anti-pTDP). Granular cytoplasmic pTDP-positive structures were observed in the CA2 area of Case 5 (K), and in the CA1 area of Case 4 (L) (anti-pTDP). Scale bar: A, C, E, and F, 10 μm; B, D, H, I, J, K, and L, 20 μm; G, 50 μm.

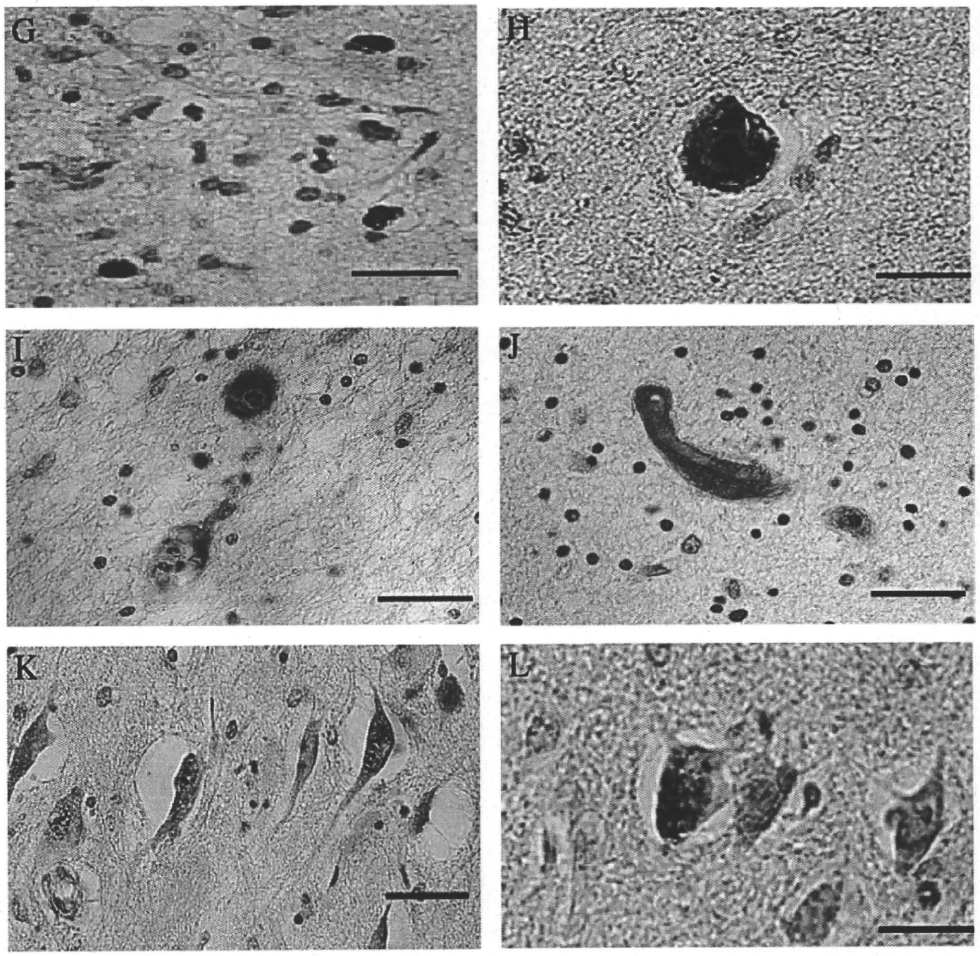

Fig. 3 (*continued*).

4.1. Alpha-Syn pathology in DNTC

The area of limbic region seemed to be the most vulnerable for aSyn pathology as well as tau pathology in DNTC (Table 1). These observations are consistent with the previous reports [21,22].

4.2. TDP-43 pathology in DNTC

We demonstrated a high frequency of TDP-43 pathology in 9 out of 10 DNTC cases (90%). Among the 9 cases having pTDP-43 pathology, 2 cases (Cases 1, 6) (22%) were identified as the 'limbic type,' while the other 7 cases (Cases 2, 3, 4, 5, 7, 8, 10) (77%) were "diffuse type," according to the classification by the study of Amador-Ortiz et al. [10]. The vulnerability of the limbic region to pTDP-43 accumulation found in our DNTC series was consistent with the previous reports of AD, DLB and AGD [10,11,13,14,23].

We mainly observed the pathology of DNTC for the purpose of comparison with FTLD. Recently, the TDP-43 pathology in FTLD has been classified into 4 subtypes according to the cortical TDP-43 pathology [24–26]. In the present study, 6 out of 7 cases (86%) with cortical TDP-43 pathology showed many NCIs/GCIs and sparse DNs, similar to the FTLD with ubiquitin-positive, tau-negative, TDP-43 positive neuronal cytoplasmic inclusions (FTLD-TDP), Type 2, using current terminology [27]. Only one case (Case 7) showed many NCI/GCIs and DNs, similarly to FTLD-TDP, Type 3. These findings of TDP-43 pathology in DNTC differ from those of AD and DLB cases, which almost all present Type 3 pathology [13,28,29].

In this point, the question arises as to whether this high frequency of TDP-43 pathology in DNTC cases represents a concurrent primary pathological process of FTLD-TDP or a secondary change occurring in susceptible neuronal populations. Although the high frequency of GCIs in DNTC is similar to the pathology of FTLD-TDP, Type 2, a simple coincidence of FTLD-TDP and DNTC seems unlikely based on our findings as follows. First, the main TDP-43 pathology in DNTC is similar to Type 2, but the frequency of TDP-43 positive NCIs in the dentate gyrus was low (one out of 9 cases; 11%) in our DNTC cases with TDP-43 immunoreactivity in comparison with those (about 80%) in FTLD-TDP, Type 2 [25,30]. Second, there are previous reports that 25–40% of FTLD-TDP cases with Type 2 pathology tend to be associated with clinical features of motor neuron disease [25,31]. In contrast, there was no case with Type 2-like pathology showing clinical features of motor neuron disease in our DNTC series.

Fig. 4. Double labeling immunofluorescence in Case 8 (A–F) demonstrates that most alpha-synuclein positive inclusions (green fluorescence in B, E) and pTDP-43 positive inclusions (red fluorescence in A, D) in the CA3 area of the hippocampus are independent (F), while there is partial colocalization of alpha-synuclein and pTDP-43 in some neuronal cytoplasmic inclusions in the deep layer of the entorhinal cortex (arrows in C). Double labeling immunofluorescence in Case 2 (G–L) demonstrates that most tau-positive neuropil threads (green fluorescence in H, K) and pTDP-43 positive inclusions (red fluorescence in G, J) in the entorhinal cortex are independent (L), while there is partial colocalization of tau and pTDP-43 in some neuronal cytoplasmic inclusions and the dentate gyrus of the hippocampus (arrows in I). Scale bar: A–L, 50 μm.

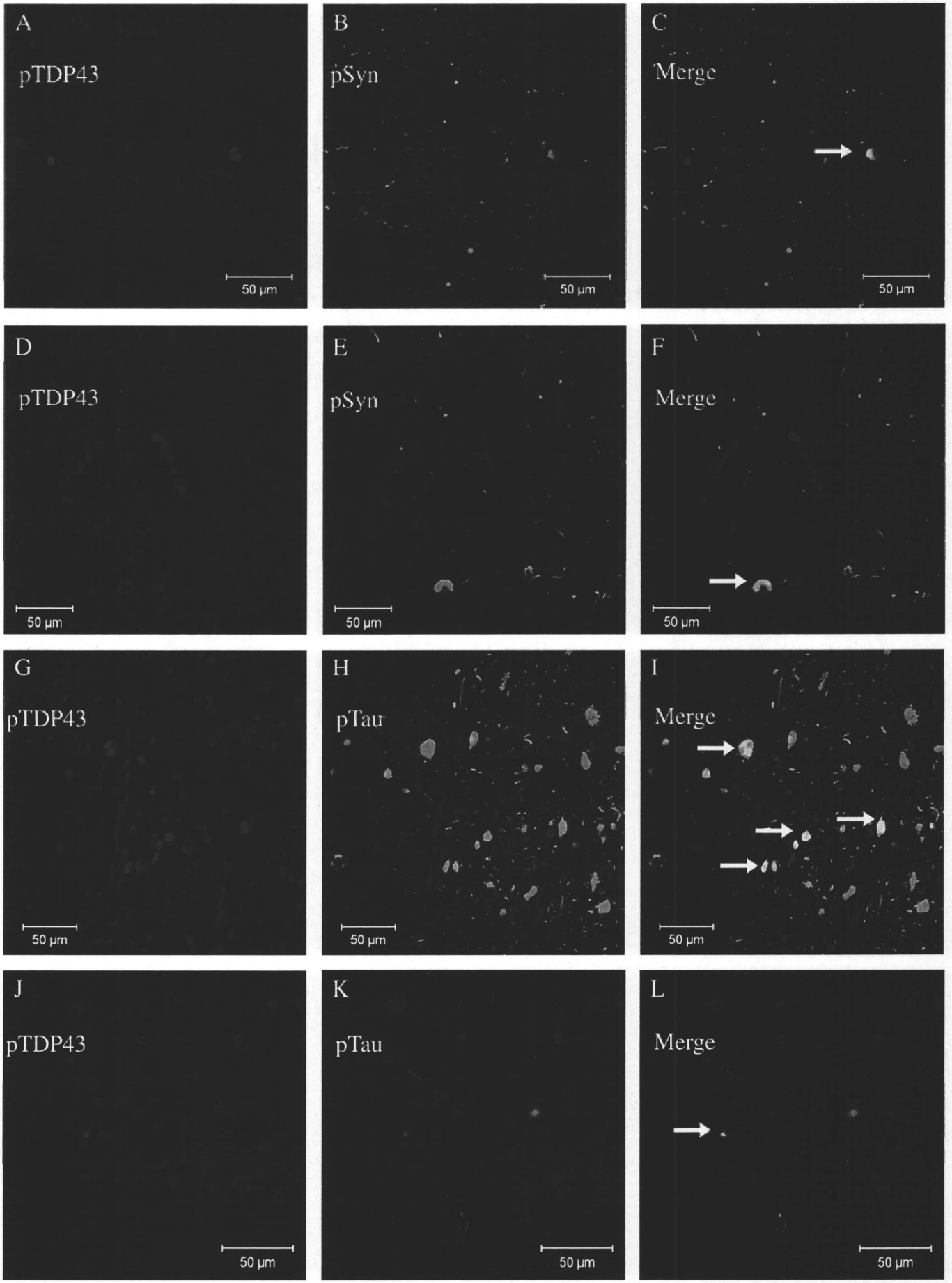
A
pTDP43
50 μm
B
pSyn
50 μm
C
Merge
50 μm
D
pTDP43
50 μm
E
pSyn
50 μm
F
Merge
50 μm
G
pTDP43
50 μm
H
pTau
50 μm
I
Merge
50 μm
J
pTDP43
50 μm
K
pTau
50 μm
L
Merge
50 μm

Therefore, it may be possible to speculate that TDP-43 pathology in DNTC has different characteristics from that of FTLD-TDP.

There arises another query concerning the possibility that the results in this study were driven by cross-reactive phospho-epitopes because the antibodies used for tau, aSyn and TDP-43 in this study were all phosphorylation-specific. Although there is some evidence of cross-reactivity with phosphorylated aSyn and phosphorylated tau [32], the anti-phosphorylated aSyn antibody used in this study did not immunostain NFT in AD brains, suggesting that it does not have cross-reactivity with phosphorylated tau.

Since the posttranslational modification is known to be a common motif in pathological protein accumulation in many neurodegenerative disorders and also this process can involve phosphorylation [33–36], the phosphorylation-dependent antibodies could mostly detect the pathological TDP-43 inclusions [13,17,37]. These mechanisms of phosphorylation might proceed in the pathologies of tau [34] or synuclein [38].

We found a scarce colocalization of pTDP-43 and tau and/or aSyn in some neuronal cytoplasmic inclusions in this study. Such a partial colocalization of tau (grain, or NFT), aSyn, and TDP-43 is consistent with that previously reported in AD, DLB, Pick's Disease, AGD, G-PDC and corticobasal degenerations to a varying degree [10–14,23]. As for the double-labeled cytoplasmic inclusions within the neuron, some reports [11,14] indicated that the TDP-43 was hardly superimposed with tau or observed only in a part of tau-positive cytoplasmic inclusions in AD or AGD based on double confocal microscopic observation. Also in this study, pTDP-43 scarcely coexisted with tau in neuronal cytoplasmic inclusions. These facts suggested that the pathway of appearance of the TDP-43 pathology might be different from that of the tau pathology but could relate closely in some way to tau proteinopathy of neurodegenerative diseases including DNTC.

It is possible that these findings were resulted from a non-specific vulnerability of the limbic region against these proteinopathies. However, there may be common factors or mechanisms that affect the conformation or modification of those proteins, leading to their intracellular accumulation. Especially, it was interesting to note that the results of the present study further supported the previous report that indicated similarity between DNTC and G-PDC [39]. Both disorders are assumed to be some type of endemic disease, and show frontotemporal atrophy and accumulation of tau, aSyn and TDP-43 without Amyloid β deposition. These findings could offer a hint toward understanding of the pathogenesis of these disorders.

4.3. Clinical features and pathology in DNTC

The phosphorylated aSyn pathology was observed in the brain stem of 5 cases of DNTC, but only one of these 5 cases had presented parkinsonism clinically. There seems to be a discrepancy between the presentation of parkinsonism and the pathological findings of phosphorylated aSyn appearance in DNTC.

There are some reports referring to an association between a specific clinical symptom and an underlying pathology in diverse degenerative disorders [40–43]. In our DNTC cases, the limbic region seemed to be the most vulnerable to abnormal accumulation of tau, aSyn and TDP-43. Thus, there is a possibility that not only accumulation of tau but also accumulation of aSyn and TDP-43 in the limbic region may be associated with early onset cognitive decline in DNTC. Indeed, in AD, concurrent TDP-43 pathology was reported to be associated with more severe cognitive decline [40].

In this study, we found a comprehensive association between pTDP-43 pathology and the frontotemporal symptoms (apathy, disinhibition, motor disturbances) in DNTC. Clinically, DNTC was diagnosed as FTLD because these three symptoms are representative and appear simultaneously to various degrees, so the integration of these three symptoms was very important for clinical assessment. Velakoulis, D. et al. recently reported that abnormalities in TDP-43 nuclear expression in the hippocampus were identified in patients with late-onset psychosis and a positive family history [44]. These findings suggest that abnormality of TDP-43 may be involved in the psychiatric symptoms of DNTC.

Meanwhile, there were some reports of DNTC without sufficient clinical or pathological assessment [4,45,46]. Cases of Fahr's syndrome with neuropsychological deficits and neuropsychiatric features have also been reported based on radiological findings [3,47,48]. More investigation will be needed to identify Fahr's syndrome as having the same background pathology of DNTC.

The association between basal ganglia calcification and psychotic symptoms has also been reported [49], but it remains unknown how the pathogenesis of calcification phenomenon concerns the psychosis. In the clinical setting, DNTC might pass unnoticed because it presents various clinical symptoms during the clinical course. Further studies on such cases from clinical, radiological and pathological standpoints might help elucidate the pathogenesis of DNTC.

5. Further assignment

We declare that there are some limitations of this study. Firstly, all the tissue samples were embedded in paraffin, so we could not perform molecular investigations including the Western Blotting test. Secondly, there were only a couple of sets of neuroimaging data of low resolution computed tomography available to this study, so we could not evaluate the association among the neuroimaging, neuropathology, and clinical symptoms. To address these issues, we are currently trying to upgrade the method for preserving tissue samples, and will acquire more neuroimaging data for a future prospective study.

References

[1] Shibayama H, Kobayashi H, Nakagawa M, Yamada K, Iwata H, Iwai K, et al. Non-Alzheimer non-Pick dementia with Fahr's syndrome. Clin Neuropathol 1992;11:237–50.
[2] Kosaka K. Diffuse neurofibrillary tangles with calcification: a new presenile dementia. J Neurol Neurosurg Psychiatry 1994;57:594–6.
[3] Modrego PJ, Mojonero J, Serrano M, Fayed N. Fahr's syndrome presenting with pure and progressive presenile dementia. Neurol Sci 2005;26:367–9.
[4] Nanda S, Bhatt SP, Pamula J, Woodruff WW, Fowler M, Miller D. Diffuse neurofibrillary tangles with calcification (DNTC): Kosaka–Shibayama disease in America. Am J Alzheimers Dis Other Demen 2007;22:535–7.
[5] Baker M, Mackenzie IR, Pickering-Brown SM, Gass J, Rademakers R, Lindholm C, et al. Mutations in progranulin cause tau-negative frontotemporal dementia linked to chromosome 17. Nature 2006;442:916–9.
[6] Cruts M, Gijselinck I, van der Zee J, Engelborghs S, Wils H, Pirici D, et al. Null mutations in progranulin cause ubiquitin-positive frontotemporal dementia linked to chromosome 17q21. Nature 2006;442:920–4.
[7] Gass J, Cannon A, Mackenzie IR, Boeve B, Baker M, Adamson J, et al. Mutations in progranulin are a major cause of ubiquitin-positive frontotemporal lobar degeneration. Hum Mol Genet 2006;15:2988–3001.
[8] Arai T, Hasegawa M, Akiyama H, Ikeda K, Nonaka T, Mori H, et al. TDP-43 is a component of ubiquitin-positive tau-negative inclusions in frontotemporal lobar degeneration and amyotrophic lateral sclerosis. Biochem Biophys Res Commun 2006;351:602–11.
[9] Neumann M, Sampathu DM, Kwong LK, Truax AC, Micsenyi MC, Chou TT, et al. Ubiquitinated TDP-43 in frontotemporal lobar degeneration and amyotrophic lateral sclerosis. Science 2006;314:130–3.
[10] Amador-Ortiz C, Lin WL, Ahmed Z, Personett D, Davies P, Duara R, et al. TDP-43 immunoreactivity in hippocampal sclerosis and Alzheimer's disease. Ann Neurol 2007;61:435–45.
[11] Higashi S, Iseki E, Yamamoto R, Minegishi M, Hino H, Fujisawa K, et al. Concurrence of TDP-43, tau and alpha-synuclein pathology in brains of Alzheimer's disease and dementia with Lewy bodies. Brain Res 2007;1184:284–94.
[12] Hasegawa M, Arai T, Akiyama H, Nonaka T, Mori H, Hashimoto T, et al. TDP-43 is deposited in the Guam parkinsonism–dementia complex brains. Brain 2007;130:1386–94.
[13] Arai T, Mackenzie IR, Hasegawa M, Nonoka T, Niizato K, Tsuchiya K, et al. Phosphorylated TDP-43 in Alzheimer's disease and dementia with Lewy bodies. Acta Neuropathol 2009;117:125–36.
[14] Fujishiro H, Uchikado H, Arai T, Hasegawa M, Akiyama H, Yokota O, et al. Accumulation of phosphorylated TDP-43 in brains of patients with argyrophilic grain disease. Acta Neuropathol 2009;117:151–8.
[15] Arai T, Kuroki N, Nizato K, Kase K, Iritani S, Ikeda K. An autopsy case of "diffuse neurofibrillary tangles with calcification", multiple infarctions and hyaline arteriosclerosis. No To Shinkei 1996;48:69–76.

[16] Shibayama H, Hoshino T, Kobayashi H, Iwase S, Takenouchi Y. An autopsy case of atypical senile dementia with atrophy of the temporal lobes—a clinical and histopathological report. Folia Psychiatr Neurol Jpn 1978;32:285–98.
[17] Hasegawa M, Arai T, Nonaka T, Kametani F, Yoshida M, Hashizume Y, et al. Phosphorylated TDP-43 in frontotemporal lobar degeneration and amyotrophic lateral sclerosis. Ann Neurol 2008;64:60–70.
[18] McKeith IG, Dickson DW, Lowe J, Emre M, O'Brien JT, Feldman H, et al. Diagnosis and management of dementia with Lewy bodies: third report of the DLB Consortium. Neurology 2005;65:1863–72.
[19] Kaufer DI, Cummings JL, Ketchel P, Smith V, MacMillan A, Shelley T, et al. Validation of the NPI-Q, a brief clinical form of the neuropsychiatric inventory. J Neuropsychiatry Clin Neurosci 2000;12:233–9.
[20] Braak H, Braak E. Neuropathological stageing of Alzheimer-related changes. Acta Neuropathol 1991;82:239–59.
[21] Yokota O, Terada S, Ishizu H, Tsuchiya K, Kitamura Y, Ikeda K, et al. NACP/alpha-synuclein immunoreactivity in diffuse neurofibrillary tangles with calcification (DNTC). Acta Neuropathol 2002;104:333–41.
[22] Hishikawa N, Hashizume Y, Ujihira N, Okada Y, Yoshida M, Sobue G. Alpha-synuclein-positive structures in association with diffuse neurofibrillary tangles with calcification. Neuropathol Appl Neurobiol 2003;29:280–7.
[23] Hu WT, Josephs KA, Knopman DS, Boeve BF, Dickson DW, Petersen RC, et al. Temporal lobar predominance of TDP-43 neuronal cytoplasmic inclusions in Alzheimer disease. Acta Neuropathol 2008;116:215–20.
[24] Sampathu DM, Neumann M, Kwong LK, Chou TT, Micsenyi M, Truax A, et al. Pathological heterogeneity of frontotemporal lobar degeneration with ubiquitin-positive inclusions delineated by ubiquitin immunohistochemistry and novel monoclonal antibodies. Am J Pathol 2006;169:1343–52.
[25] Mackenzie IR, Baborie A, Pickering-Brown S, Du Plessis D, Jaros E, Perry RH, et al. Heterogeneity of ubiquitin pathology in frontotemporal lobar degeneration: classification and relation to clinical phenotype. Acta Neuropathol 2006;112:539–49.
[26] Cairns NJ, Bigio EH, Mackenzie IR, Neumann M, Lee VM, Hatanpaa KJ, et al. Neuropathologic diagnostic and nosologic criteria for frontotemporal lobar degeneration: consensus of the Consortium for Frontotemporal Lobar Degeneration. Acta Neuropathol 2007;114:5–22.
[27] Mackenzie IR, Neumann M, Bigio EH, Cairns NJ, Alafuzoff I, Kril J, et al. Nomenclature for neuropathologic subtypes of frontotemporal lobar degeneration: consensus recommendations. Acta Neuropathol 2009;117:15–8.
[28] Nakashima-Yasuda H, Uryu K, Robinson J, Xie SX, Hurtig H, Duda JE, et al. Co-morbidity of TDP-43 proteinopathy in Lewy body related diseases. Acta Neuropathol 2007;114:221–9.
[29] Uryu K, Nakashima-Yasuda H, Forman MS, Kwong LK, Clark CM, Grossman M, et al. Concomitant TAR-DNA-binding protein 43 pathology is present in Alzheimer disease and corticobasal degeneration but not in other tauopathies. J Neuropathol Exp Neurol 2008;67:555–64.
[30] Davidson Y, Amin H, Kelley T, Shi J, Tian J, Kumaran R, et al. TDP-43 in ubiquitinated inclusions in the inferior olives in frontotemporal lobar degeneration and in other neurodegenerative diseases: a degenerative process distinct from normal ageing. Acta Neuropathol 2009;118:359–69.
[31] Josephs KA, Stroh A, Dugger B, Dickson DW. Evaluation of subcortical pathology and clinical correlations in FTLD-U subtypes. Acta Neuropathol 2009;118:349–58.
[32] Piao YS, Hayashi S, Hasegawa M, Wakabayashi K, Yamada M, Yoshimoto M, et al. Co-localization of alpha-synuclein and phosphorylated tau in neuronal and glial cytoplasmic inclusions in a patient with multiple system atrophy of long duration. Acta Neuropathol 2001;101:285–93.
[33] Ferrer I, Gomez-Isla T, Puig B, Freixes M, Ribe E, Dalfo E, et al. Current advances on different kinases involved in tau phosphorylation, and implications in Alzheimer's disease and tauopathies. Curr Alzheimer Res 2005;2:3–18.
[34] Luna-Munoz J, Chavez-Macias L, Garcia-Sierra F, Mena R. Earliest stages of tau conformational changes are related to the appearance of a sequence of specific phospho-dependent tau epitopes in Alzheimer's disease. J Alzheimers Dis 2007;12:365–75.
[35] Obi K, Akiyama H, Kondo H, Shimomura Y, Hasegawa M, Iwatsubo T, et al. Relationship of phosphorylated alpha-synuclein and tau accumulation to Abeta deposition in the cerebral cortex of dementia with Lewy bodies. Exp Neurol 2008;210:409–20.
[36] Cook C, Zhang YJ, Xu YF, Dickson DW, Petrucelli L. TDP-43 in neurodegenerative disorders. Expert Opin Biol Ther 2008;8:969–78.
[37] Schwab C, Arai T, Hasegawa M, Yu S, McGeer PL. Colocalization of transactivation-responsive DNA-binding protein 43 and huntingtin in inclusions of Huntington disease. J Neuropathol Exp Neurol 2008;67:1159–65.
[38] Saito Y, Kawashima A, Ruberu NN, Fujiwara H, Koyama S, Sawabe M, et al. Accumulation of phosphorylated alpha-synuclein in aging human brain. J Neuropathol Exp Neurol 2003;62:644–54.
[39] Tanabe Y, Ishizu H, Ishiguro K, Itoh N, Terada S, Haraguchi T, et al. Tau pathology in diffuse neurofibrillary tangles with calcification (DNTC): biochemical and immunohistochemical investigation. NeuroReport 2000;11:2473–7.
[40] Josephs KA, Whitwell JL, Knopman DS, Hu WT, Stroh DA, Baker M, et al. Abnormal TDP-43 immunoreactivity in AD modifies clinicopathologic and radiologic phenotype. Neurology 2008;70:1850–7.
[41] Yokota O, Tsuchiya K, Arai T, Yagishita S, Matsubara O, Mochizuki A, et al. Clinicopathological characterization of Pick's disease versus frontotemporal lobar degeneration with ubiquitin/TDP-43-positive inclusions. Acta Neuropathol 2009;117:429–44.
[42] Grossman M. Primary progressive aphasia: clinicopathological correlations. Nat Rev Neurol 2010; 6:88–97.
[43] Deramecourt V, Lebert F, Debachy B, Mackowiak-Cordoliani MA, Bombois S, Kerdraon O, et al. Prediction of pathology in primary progressive language and speech disorders. Neurology 2010; 74:42–49.
[44] Velakoulis D, Walterfang M, Mocellin R, Pantelis C, Dean B, McLean C. Abnormal hippocampal distribution of TDP-43 in patients with-late onset psychosis. Aust N Z J Psychiatry 2009;43:739–45.
[45] Nomoto N, Sugimoto H, Iguchi H, Kurihara T, Wakata N. A case of Fahr's disease presenting "diffuse neurofibrillary tangles with calcification". Rinsho Shinkeigaku 2002;42:745–9.
[46] Langlois NE, Grieve JH, Best PV. Changes of diffuse neurofibrillary tangles with calcification (DNTC) in a woman without evidence of dementia. J Neurol Neurosurg Psychiatry 1995;59:103.
[47] Hempel A, Henze M, Berghoff C, Garcia N, Ody R, Schroder J. PET findings and neuropsychological deficits in a case of Fahr's disease. Psychiatry Res 2001;108:133–40.
[48] Konupcikova K, Masopust J, Valis M, Horacek J. Dementia in a patient with Fahr's syndrome. Neuro Endocrinol Lett 2008;29:431–4.
[49] Ostling S, Andreasson LA, Skoog I. Basal ganglia calcification and psychotic symptoms in the very old. Int J Geriatr Psychiatry 2003;18:983–7.

Journal of the Neurological Sciences 300 (2011) 9–13

Contents lists available at ScienceDirect

Journal of the Neurological Sciences

journal homepage: www.elsevier.com/locate/jns

FALS with Gly72Ser mutation in SOD1 gene: Report of a family including the first autopsy case

Zen Kobayashi [a,b,*], Kuniaki Tsuchiya [a], Takayuki Kubodera [b], Noriyuki Shibata [c], Tetsuaki Arai [a,d], Hiroyuki Miura [e], Chieko Ishikawa [f], Hiromi Kondo [a], Hideki Ishizu [g], Haruhiko Akiyama [a], Hidehiro Mizusawa [b]

[a] Department of Psychogeriatrics, Tokyo Institute of Psychiatry, 2-1-8 Kamikitazawa, Setagaya-ku, Tokyo, 156-8585, Japan
[b] Department of Neurology and Neurological Science, Graduate School, Tokyo Medical and Dental University, Tokyo, 113-8519, Japan
[c] Department of Pathology, Tokyo Women's Medical University, Tokyo, 162-8666, Japan
[d] Department of Psychiatry, Graduate School of Comprehensive Human Sciences, University of Tsukuba, Ibaraki, 305-8575, Japan
[e] Department of Internal medicine, Ichihara Hospital, Ibaraki, 300-3295, Japan
[f] Department of Neurology, Chiba-East National Hospital, Chiba, 260-8712, Japan
[g] Department of Laboratory Medicine, Zikei Institute of Psychiatry, Okayama, 702-8508, Japan

ARTICLE INFO

Article history:
Received 31 August 2010
Received in revised form 23 October 2010
Accepted 28 October 2010
Available online 16 November 2010

Keywords:
Familial amyotrophic lateral sclerosis (FALS)
Cu/Zn superoxide dismutase-1 (SOD1)
Gly72Ser
Onuf's nucleus
Hyaline inclusion

ABSTRACT

Clinical information on familial amyotrophic lateral sclerosis (FALS) with Gly72Ser mutation in the Cu/Zn superoxide dismutase-1 (SOD1) gene has been limited and autopsy findings remain to be clarified. We describe one Japanese family with ALS carrying Gly72Ser mutation in the SOD1 gene, in which autopsy was performed on one affected member. The autopsied female patient developed muscle weakness of the left thigh at age 66 and showed transient upper motor neuron signs. She died of respiratory failure 13 months after onset without artificial respiratory support. There were no symptoms suggesting bladder or rectal dysfunction throughout the clinical course. Her brother with ALS was shown to have Gly72Ser mutation in the SOD1 gene. Histopathologically, motor neurons were markedly decreased throughout the whole spinal cord, whereas corticospinal tract involvement was very mild and was demonstrated only by CD68 immunohistochemistry. Degeneration was evident in the posterior funiculus, Clarke's nucleus, posterior cerebellar tract, and Onuf's nucleus. Neuronal hyaline inclusions were rarely observed in the neurons of the spinal cord anterior horn including Onuf's nucleus, and were immunoreactive for SOD1. To date, neuron loss in Onuf's nucleus has hardly been seen in ALS, except in the patients showing prolonged disease duration with artificial respiratory support. Involvement of Onuf's nucleus may be a characteristic pathological feature in FALS with Gly72Ser mutation in the SOD1 gene.

1. Introduction

Amyotrophic lateral sclerosis (ALS) is a fatal neurodegenerative disorder that mainly involves the upper and lower motor neurons. Familial cases account for 5–10% of all cases of ALS, and mutations of the Cu/Zn superoxide dismutase-1 (SOD1) gene, which encodes an antioxidant enzyme, are present in about 20% of FALS patients and in about 2% of sporadic ALS (SALS) patients [1]. Over 150 mutations in the SOD1 gene have been identified in FALS and SALS cases since 1993 [2]. Within the cell, SOD1 is physiologically distributed in the cytosol, lysosomes, microsomes, mitochondria, and nuclei [3]. Misfolding and aggregation of SOD1 is related to gain of toxic function in ALS with SOD1 mutation [4]. Increasing evidence indicates that non-neuronal-neighboring cell types contribute to the pathogenesis and disease progression [5].

Clinical features of ALS with SOD1 mutation are largely indistinguishable from those of SALS; however, lower limb-onset and lower motor neuron-predominant involvement are relatively common [6]. The onset age and disease duration are variable among the mutations. Histopathologically, most cases of ALS with SOD1 mutation show Lewy body-like hyaline inclusions, which are immunoreactive for SOD1 [7–9]. The posterior funiculus, Clarke's nucleus and posterior spinocerebellar tract were also involved. The corticospinal tract (CST) involvement is slight or mild [7]. In patients with the I113T mutation, neurofilament pathology is an almost universal feature [7].

Onuf's nucleus is a small group of cells, first described by a neuroanatomist called Onufrowicz. In 1899, he found that this group of cells was localized exclusively in the second sacral segment [10]. Onuf's nucleus is functionally related to the rectum and bladder, including the external sphincter muscles of the anus and urethra [10].

* Corresponding author. Department of Psychogeriatrics, Tokyo Institute of Psychiatry, 2-1-8 Kamikitazawa, Setagaya-ku, Tokyo, 156-8585, Japan.
E-mail address: zen@bg7.so-net.ne.jp (Z. Kobayashi).

0022-510X/$ – see front matter © 2010 Elsevier B.V. All rights reserved.
doi:10.1016/j.jns.2010.10.030

Onuf's nucleus is usually preserved in ALS [10,11], and neuron loss has hardly been seen except in the patients showing prolonged disease duration with artificial respiratory support [12–15]. Here, we report one Japanese family with ALS showing Gly72Ser mutation including the first autopsy patient, in whom both neuron loss and neuronal cytoplasmic inclusions were demonstrated in Onuf's nucleus.

2. Clinical assessment

2.1. Case II-2

The family tree is shown in Fig. 1. A 75-year-old Japanese man developed muscle weakness of the fingers of the bilateral upper limbs. There had been paresis of the right upper limb since brain infarction occurred at age 65. Two patients with ALS in his family had already died (Fig. 1). Six months after onset, muscle weakness emerged at the proximal parts of the bilateral upper limbs, and nine months after onset, he became unable to produce vocal sounds. He was admitted to the Department of Neurology in the general hospital ten months after onset. On admission, there was marked tongue atrophy and fasciculation, and prominent dysarthria. Neck weakness corresponded to grade 3 in the manual muscle testing. Symmetrical muscle weakness of the bilateral upper limbs ranged from grades 3 to 4 on manual muscle testing. There was no muscle weakness in the lower limbs. Deep tendon reflex was increased in the right upper limb and bilateral lower limbs. Plantar reflexes were not elicited. There was no sensory disturbance. Needle electromyography detected active and chronic denervation potentials, and a diagnosis of familial ALS was made. DNA was extracted from his blood sample, and direct sequencing of SOD1 gene exon 3 showed missense mutation substituting glycine for serine (Gly72Ser) (Fig. 2). He died of respiratory failure ten months after onset. Autopsy could not be performed.

2.2. Case II-4

A 66-year-old woman developed muscle weakness of the left thigh, and experienced falls. Two months after onset, fasciculation emerged in the muscles of the left thigh. Four months after onset, she needed a cane while walking, then became unable to walk and was admitted to a general hospital five months after onset. On admission, there were muscle fasciculations in the bilateral thigh and hip, and muscle atrophy and weakness in the left lower limb. Muscle weakness ranged from grades 0 to 2 on manual muscle testing. Achilles tendon reflex was absent on the left side, and was within normal limits on the right. The patellar tendon reflex was decreased on the left side and increased on the right. The upper limbs tendon reflex was bilaterally increased. There was Babinski's sign bilaterally. Vibration sensation was slightly decreased in the bilateral lower limbs. On nerve conduction study, there was no conduction block. Needle electromyography showed denervation potentials in the bilateral lower limbs and right upper limb. A diagnosis of ALS was made. At that time, information on the family history of ALS could not be obtained. Thereafter, muscle weakness emerged in the right lower limb.

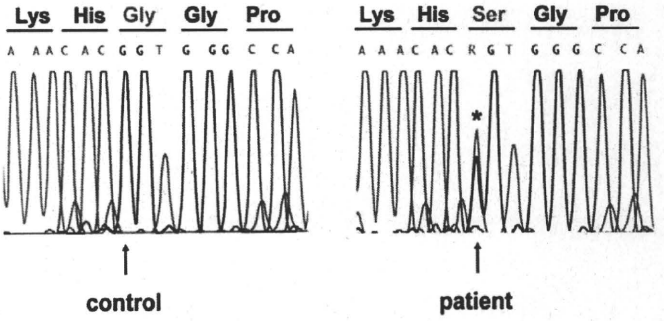

Fig. 2. Direct sequencing of SOD1 gene exon 3 showed missense mutation substituting glycine for serine (Gly72Ser).

Seven months after onset, neurological examination demonstrated flaccid paraparesis without hyperreflexia or plantar reflexes. Nerve conduction study demonstrated reduction of the amplitude of the compound muscle action potentials (CMAPs), but conduction velocity was within normal limits. Cerebrospinal fluid examination showed slight elevation of the total protein level (53 mg/dl). Because we could not completely exclude the possibility of chronic inflammatory demyelinating polyradiculoneuropathy (CIDP), prednisolone of 60 mg was administered for six months. However, there was no improvement.

About ten months after onset, muscle weakness emerged in the trunk and upper limbs, and non-invasive positive pressure ventilation was initiated. At that time, neurological examination demonstrated lower-limb dominant tetraparesis and absence of the tendon reflex in the bilateral lower limbs. There was no facial palsy, dysarthria, dysphasia, or tongue atrophy. Nerve conduction study demonstrated marked reduction of the amplitude of the CMAPs in the four limbs (<0.3 mV), but conduction velocity remained within normal limits. Muscle action potentials were not detected in the right tibial nerve or left ulnar nerve. Sensory nerve action potentials (SNAPs) were within normal limits. The patient refused artificial respiratory support and died of respiratory failure 13 months after onset. There were no symptoms suggesting bladder or rectal dysfunction throughout the clinical course. Genetic sequencing could not be performed.

2.3. Case II-6

This patient was also diagnosed as having ALS and died at age 39, but information other than this could not be obtained.

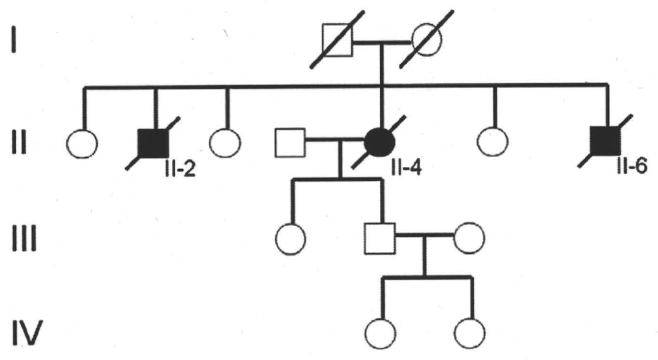

Fig. 1. Pedigree of a Japanese family with FALS harboring Gly72Ser mutation in the SOD1 gene. Males are represented by square, females by circles. Affected members are represented by solid symbols, deceased individuals by diagonals.

Table 1
Antibodies used for immunohistochemistry.

Antibody	Type	Source	Dilution
Anti-ubiquitin	Rabbit polyclonal	Dako, Glostrup, Denmark	1:2000
Anti-p62 (SQSTM1)	Rabbit polyclonal	Biomol, Philadelphia, PA, USA	1:1000
Anti-TDP-43	Rabbit polyclonal	Proteintech Group, Chicago, IL, USA	1:1000
Anti-SOD1	Rabbit polyclonal	Made by Asayama et al. [21]	1:20,000
Anti-neurofilament (SMI 31)	Mouse monoclonal	Sternberger, Lutherville, MD, USA	1:1000
Anti-CD68	Mouse monoclonal	Dako, Glostrup, Denmark	1:100

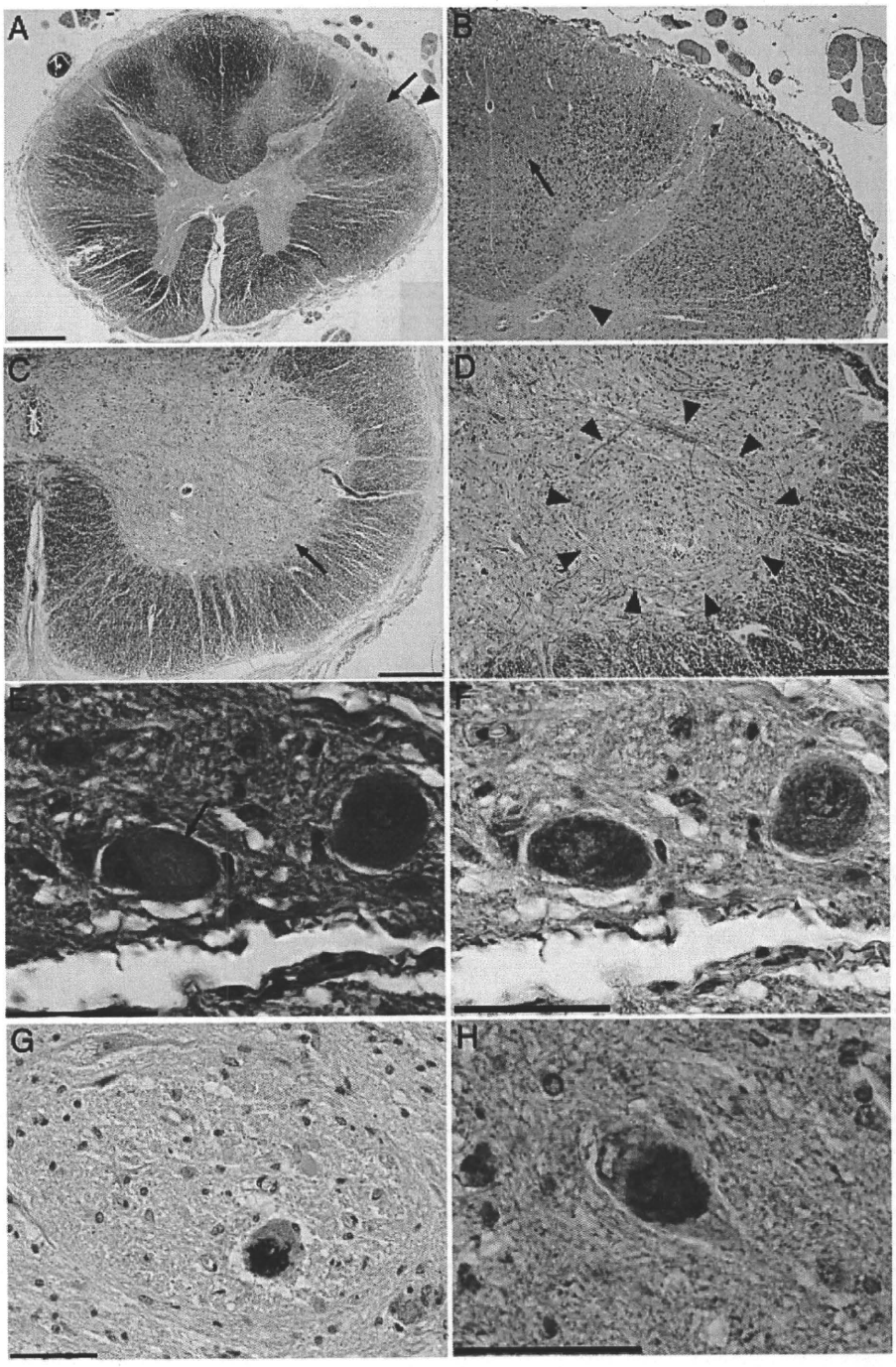

Fig. 3. (A) and (B) are serial sections. A. In the lower thoracic cord, the central portion of the posterior funiculus was involved with left predominance, and the posterior intermediate sulci could not be identified. Although the subpial region was not well stained by KB staining, myelin pallor was evident in the posterior cerebellar tract (arrowhead). The corticospinal tract (CST) involvement was not apparent (arrow). B. CD68 immunohistochemistry of the left lateral and posterior funiculi showed proliferation of activated macrophages/microglia in the CST, Clarke's nucleus (arrowhead), posterior cerebellar tract and posterior funiculus. In the posterior funiculus, the region around the posterior central sulcus (arrow) was almost intact. C. Marked neuronal loss was observed in the anterior horn of the left second sacral segment. The arrow indicates Onuf's nucleus. D. A high-power view of the left Onuf's nucleus (arrowheads) demonstrated severe neuron loss. E, F. The hyaline inclusion (E, arrow) in a neuron of Onuf's nucleus demonstrated by HE staining was partially immunoreactive for SOD1 (F). The nucleus was located in the periphery. G. The left Onuf's nucleus is shown. Using p62 immunohistochemistry, the inclusion in the remaining neuron of Onuf's nucleus were labeled. H. The other inclusion immunoreactive for SOD1 in the remaining neuron of the anterior horn of the second sacral segment. Scale bars = 1 mm (A), 500 μm (C), 200 μm (D), and 50 μm (E-H).

3. Methods

Brain and spinal cord tissue samples of case II-4 were fixed postmortem with 10% formalin and embedded in paraffin. Ten-micrometer-thick (Multiple 10-μm-thick) sections were prepared from the cerebrum, midbrain, pons, medulla oblongata, cerebellum, and spinal cord including the cervical, thoracic, lumbar and sacral segments. These sections were stained with hematoxylin–eosin (HE) and Klüver-Barrera (KB) and by the Bodian impregnation method. Spinal cord sections were examined immunohistochemically by the immunoperoxidase method using 3,3′-diaminobenzidine tetrahydrochloride and hematoxylin as the chromogen and counterstain, respectively. Antibodies used in this study are shown in Table 1.

Table 2
Clinical features of familial amyotrophic lateral sclerosis with Gly72Ser mutation in the SOD1 gene.

	Age at onset/Gender	Age at death	Site of onset	Atypical features	Disease penetrance in the family
Orrell et al. III-3 [16]	47/M	51	Right foot	Decreased vibration sensation, No UMN signs	Incomplete
Orrell et al. III-8 [16]	46 or 47/F	49	Legs	ND	
Shaw et al. [17]	29/M	30 or 31	Left thigh	No family history	Incomplete
Present case II-2	75/M	76	Upper limbs	ND	Incomplete
Present case II-4	66/F	67	Left thigh	Decreased vibration sensation, Limited UMN signs	
Present case II-6	ND/M	39	ND	ND	

M male, *F* female, *UMN* upper motor neuron, *ND* not described.

4. Results

4.1. Neuropathological findings

Brain weight was 1225 g after fixation. Macroscopically, there were no abnormalities in the brain. The anterior roots of the spinal cord were atrophic. Microscopically, as previously reported in ALS cases showing SOD1 mutation, the posterior funiculus was involved throughout the whole spinal cord, and the posterior cerebellar tract was also affected in the thoracic and cervical cord (Fig. 3A, B). In the thoracic cord, neurons of Clarke's nucleus were depleted, whereas the intermediolateral nucleus was preserved. The CST involvement was not apparent by KB staining (Fig. 3A). Severe neuron loss was observed in the anterior horn of the whole spinal cord (Fig. 3C). The number of neurons in Onuf's nucleus were slightly decreased on the right side, and markedly decreased on the left (Fig. 3D). This finding was confirmed on ten serial sections. Neuronal hyaline inclusions were rarely observed in the remaining neurons of the spinal cord anterior horn including Onuf's nucleus (Fig. 3E). There were no apparent astrocytic hyaline inclusions [13]. In the brainstem, neuronal loss was slight in the hypoglossal nucleus, and was not apparent in the motor nucleus of the trigeminal nerve. There were no Bunina bodies. There was no apparent neuronal loss in the cerebrum or cerebellum including the primary motor cortex, although the neurons in these regions frequently showed ischemic changes related to hypoxia in the terminal stage of the disease.

4.2. Immunohistochemical findings

Although the CST involvement was not apparent by myelin stain as described above, CD68 immunohistochemistry demonstrated proliferation of activated macrophages/microglia in the CST (Fig. 3B). CD68 immunohistochemistry also showed involvement of the posterior cerebellar tract, Clarke's nucleus (Fig. 3B), and inferior cerebellar peduncle of the medulla oblongata. Ubiquitin, p62, and SOD1 immunohistochemistry demonstrated neuronal cytoplasmic inclusions in the remaining neurons of the spinal cord anterior horn including Onuf's nucleus (Fig. 3F–H). Immunoreactivity for neurofilament or TDP-43 was not apparent in the inclusions. Onuf's nucleus sections containing hyaline inclusions were first stained with HE, and photographed, and then destained in ethanol, and finally immunostained for SOD1. Hyaline inclusions in the remaining neurons of Onuf's nucleus identified by HE staining (Fig. 3E) were partially and irregularly imunoreactive for SOD1 (Fig. 3F).

5. Discussion

The clinical features of FALS with Gly72 Ser mutation in the SOD1 gene is summarized in Table 2. Unlike previous reports [16,17], our cases II-2 and II-4 showed disease onset in the sixth or seventh decade. In addition, case II-2 developed weakness of the upper limbs, and the lower limbs were well preserved throughout the clinical course. These findings indicate that the same Gly72Ser mutation may present different clinical courses, even within the same family. In case II-4 (autopsied patient), neurological examination had shown decreased vibration sensation in the lower limbs although the patient did not complain of sensory symptoms. Additionally, we could not clinically exclude the possibility of CIDP in this patient because the upper motor neuron signs were limited. In the view of clinicopathological correlation, impaired vibration sensation may be due to posterior funiculus involvement, and limited upper motor neuron signs appeared to reflect mild CST involvement.

Neuropathologically, many SOD1-mutated FALS cases show neuronal Lewy body-like hyaline inclusions. In addition, long surviving FALS patients with SOD1 gene mutations present with astrocytic hyaline inclusions [7]. These neuronal and astrocytic inclusions contain both wild-type and mutant SOD1 protein. In some mutations, however, SOD1 aggregation is not demonstrated histopathologically [7], therefore the process of neuron death may somewhat differ among the mutations. Further study is required to clarify the process of neuronal degeneration in ALS with SOD1 mutation.

The salient pathological feature in case II-4 was neuron loss in Onuf's nucleus, although clinical symptoms suggesting bladder or rectal dysfunction were absent. SOD1 aggregation demonstrated in the remaining neurons of Onuf's nucleus suggests that Onuf's nucleus was involved in the disease process associated with Gly72Ser mutation. To date, Onuf's nucleus has been considered largely intact in ALS [10,11], and neuron loss has hardly been seen except in patients showing prolonged disease duration with artificial respiratory support [12–15]. Exceptionally, Yoshida et al [18] and Kihira et al [19] reported a FALS case and a SALS case respectively, showing neuron loss in Onuf's nucleus despite disease duration shorter than three years. In the other study, Kihira et al. showed Bunina bodies and ubiquitin-immunoreactive inclusions in the neurons of Onuf's nucleus in some ALS cases while neuron loss was not apparent [20]. They concluded that Onuf's nucleus is involved in the disease process in some ALS cases, although the severity of degeneration was of a lesser degree than that in other motor nuclei. Among ALS cases showing the SOD1 mutation, neuron loss with neuronal and glial inclusions in Onuf's nucleus was reported only in one patient with two base pair deletion in codon 126 of exon 5 [13], who showed a prolonged disease duration with artificial respiratory support.

In conclusion, the findings in this family provide new information regarding the clinicopathological features of FALS with Gly72Ser mutation in the SOD1 gene. Further clinicopathological information in a larger number of cases showing Gly72Ser mutation is needed to clarify whether involvement of Onuf's nucleus is associated with this mutation.

Acknowledgements

This work was supported by Grants-in-Aid from the Ministry of Health, Labour and Welfare of Japan, Grants-in-Aid for scientific research from the Ministry of Education, Culture, Sports, Science and Technology (14570957) and a research grant from the Zikei Institute of Psychiatry.

References

[1] Wijesekera LC, Leigh PN. Amyotrophic lateral sclerosis. Orphanet J Rare Dis 2009;4:3.

[2] Battistini S, Ricci C, Lotti EM, Benigni M, Gagliardi S, Zucco R, et al. Severe familial ALS with a novel exon 4 mutation (L106F) in the SOD1 gene. J Neurol Sci 2010;293:112–5.

[3] Okado-Matsumoto A, Fridovich I. Subcellular distribution of superoxide dismutases (SOD) in rat liver: Cu,Zn-SOD in mitochondria. J Biol Chem 2001;276: 38388–93.

[4] Kerman A, Liu HN, Croul S, Bilbao J, Rogaeva E, Zinman L, et al. Amyotrophic lateral sclerosis is a non-amyloid disease in which extensive misfolding of SOD1 is unique to the familial form. Acta Neuropathol 2010;119:335–44.

[5] Ilieva H, Polymenidou M, Cleveland DW. Non-cell autonomous toxicity in neurodegenerative disorders: ALS and beyond. J Cell Biol 2009;187:761–72.

[6] Aoki M, Warita H, Itoyama Y. Amyotrophic lateral sclerosis with the SOD1 mutations. Rinsho Shinkeigaku 2008;48:966–9.

[7] Kato S. Amyotrophic lateral sclerosis models and human neuropathology: similarities and differences. Acta Neuropathol 2008;115:97–114.

[8] Shibata N, Hirano A, Kobayashi M, Siddique T, Deng HX, Hung WY, et al. Intense superoxide dismutase-1 immunoreactivity in intracytoplasmic hyaline inclusions of familial amyotrophic lateral sclerosis with posterior column involvement. J Neuropathol Exp Neurol 1996;55:481–90.

[9] Shibata N, Hirano A, Yamamoto T, Kato Y, Kobayashi M. Superoxide dismutase-1 mutation-related neurotoxicity in familial amyotrophic lateral sclerosis. Amyotroph Lateral Scler Other Mot Neuron Disord 2000;1:143–61.

[10] Mannen T. Neuropathological findings of Onuf's nucleus and its significance. Neuropathology 2000;20:S30–3.

[11] Mannen T, Iwata M, Toyokura Y, Nagashima K. Preservation of a certain motoneurone group of the sacral cord in amyotrophic lateral sclerosis: its clinical significance. J Neurol Neurosurg Psychiatry 1977;40:464–9.

[12] Kato S, Hayashi H, Oda M, Kawata A, Shimizu T, Hayashi M, et al. Neuropathology in sporadic ALS patients on respirators. In: Nakano I, Hirano A, editors. Amyotrophic Lateral Sclerosis :Progress and Perspectives in Basic Research and Clinical Application. Amsterdam: Elsevier; 1996. p. 66–77.

[13] Kato S, Shimoda M, Watanabe Y, Nakashima K, Takahashi K, Ohama E. Familial amyotrophic lateral sclerosis with a two base pair deletion in superoxide dismutase 1: gene multisystem degeneration with intracytoplasmic hyaline inclusions in astrocytes. J Neuropathol Exp Neurol 1996;55:1089–101.

[14] Shimizu T, Kawata A, Kato S, Hayashi M, Takamoto K, Hayashi H, et al. Autonomic failure in ALS with a novel SOD1 gene mutation. Neurology 2000;54:1534–7.

[15] Tateishi T, Hokonohara T, Yamasaki R, Miura S, Kikuchi H, Iwaki A, et al. Multiple system degeneration with basophilic inclusions in Japanese ALS patients with FUS mutation. Acta Neuropathol 2010;119:355–64.

[16] Orrell RW, Marklund SL, deBelleroche JS. Familial ALS is associated with mutations in all exons of SOD1: a novel mutation in exon 3 (Gly72Ser). J Neurol Sci 1997;153: 46–9.

[17] Shaw CE, Enayat ZE, Chioza BA, Al-Chalabi A, Radunovic A, Powell JF, et al. Mutations in all five exons of SOD-1 may cause ALS. Ann Neurol 1998;43:390–4.

[18] Yoshida M, Okuda S, Murakami N, Hashizume Y, Sobue G. Two siblings of familial amyotrophic lateral sclerosis with multisystemic degeneration characterized by mild involvement of the middle root zone of the posterior column, Clarke's nuclei and spinocerebellar tract. Rinsho Shinkeigaku 1995;35:589–99.

[19] Kihira T, Mizusawa H, Tada J, Namikawa T, Yoshida S, Yase Y. Lewy body-like inclusions in Onuf's nucleus from two cases of sporadic amyotrophic lateral sclerosis. J Neurol Sci 1993;115:51–7.

[20] Kihira T, Yoshida S, Yoshimasu F, Wakayama I, Yase Y. Involvement of Onuf's nucleus in amyotrophic lateral sclerosis. J Neurol Sci 1997;147:81–8.

[21] Asayama K, Janco RL, Burr IM. Selective induction of manganous superoxide dismutase in human monocytes. Am J Physiol 1985;249:C393–7.

THE JOURNAL OF BIOLOGICAL CHEMISTRY VOL. 285, NO. 45, pp. 34885–34898, November 5, 2010

Seeded Aggregation and Toxicity of α-Synuclein and Tau

CELLULAR MODELS OF NEURODEGENERATIVE DISEASES[*] [S]

Received for publication, May 26, 2010, and in revised form, August 17, 2010 Published, JBC Papers in Press, August 30, 2010, DOI 10.1074/jbc.M110.148460

Takashi Nonaka[‡1], **Sayuri T. Watanabe**[‡§], **Takeshi Iwatsubo**[§¶], **and Masato Hasegawa**[‡2]

From the [‡]*Department of Molecular Neurobiology, Tokyo Institute of Psychiatry, Tokyo 156-8585 and the* [§]*Department of Neuropathology and Neuroscience, Graduate School of Pharmaceutical Science, and* [¶]*Department of Neuropathology, Graduate School of Medicine, University of Tokyo, Tokyo 113-0033, Japan*

The deposition of amyloid-like filaments in the brain is the central event in the pathogenesis of neurodegenerative diseases. Here we report cellular models of intracytoplasmic inclusions of α-synuclein, generated by introducing nucleation seeds into SH-SY5Y cells with a transfection reagent. Upon introduction of preformed seeds into cells overexpressing α-synuclein, abundant, highly filamentous α-synuclein-positive inclusions, which are extensively phosphorylated and ubiquitinated and partially thioflavin-positive, were formed within the cells. SH-SY5Y cells that formed such inclusions underwent cell death, which was blocked by small molecular compounds that inhibit β-sheet formation. Similar seed-dependent aggregation was observed in cells expressing four-repeat Tau by introducing four-repeat Tau fibrils but not three-repeat Tau fibrils or α-synuclein fibrils. No aggregate formation was observed in cells overexpressing three-repeat Tau upon treatment with four-repeat Tau fibrils. Our cellular models thus provide evidence of nucleation-dependent and protein-specific polymerization of intracellular amyloid-like proteins in cultured cells.

The conversion of certain soluble peptides and proteins into insoluble filaments or misfolded amyloid proteins is believed to be the central event in the etiology of a majority of neurodegenerative diseases (1–4). Alzheimer disease (AD)[3] is characterized by the deposition of two kinds of filamentous aggregates, extracellular deposits of β-amyloid plaques composed of amyloid β (Aβ) peptides, and intracellular neurofibrillary lesions consisting of hyperphosphorylated Tau. In Parkinson disease (PD) and dementia with Lewy bodies (DLB), filamentous inclusions consisting of hyperphosphorylated α-synuclein (α-syn) are accumulated in degenerating neurons (5). The deposition of prion proteins in synapses and extracellular spaces is the defining characteristic of Creutzfeldt-Jakob disease and other prion diseases (3). The identification of genetic defects associated with early onset AD, familial PD, frontotemporal dementia, parkinsonism linked to chromosome 17 (caused by Tau mutation and deposition), and familial Creutzfeldt-Jakob disease has led to the hypothesis that the production and aggregation of these proteins are central to the development of neurodegeneration. Fibrils formed of Aβ display a prototypical cross-β-structure characteristic of amyloid (6), as do many other types of filaments deposited in the extracellular space in systemic or organ-specific amyloidoses (7), including prion protein deposits (8). Filaments assembled from α-syn (9) and from Tau filaments (10) were also shown to possess cross-β-structure, as were synthetic filaments derived from exon 1 of huntingtin with 51 glutamines (11). It therefore seems appropriate to consider neurodegenerative disorders developing intracellular deposits of amyloid-like proteins as brain amyloidosis. The accumulation and propagation of extracellular amyloid proteins are believed to occur through nucleation-dependent polymerization (12, 13). However, it has been difficult to establish the relevance of this process in the *in vivo* situation because of the lack of a suitable cell culture model or method to effectively introduce seeds into cells. For example, it has not yet been possible to generate *bona fide* fibrous inclusions reminiscent of Lewy bodies as a model of PD by overexpressing α-syn in neurons of transgenic animals. Here, we describe a novel method for introducing amyloid seeds into cultured cells using lipofection, and we present experimental evidence of seed-dependent polymerization of α-syn, leading to the formation of filamentous protein deposits and cell death. This was also clearly demonstrated in cells expressing different Tau isoforms by introducing the corresponding Tau fibril seeds.

EXPERIMENTAL PROCEDURES

Chemicals and Antibodies—A phosphorylation-independent antibody Syn102 and monoclonal and polyclonal antibodies against a synthetic phosphopeptide of α-syn (Ser(P)[129]) were used as described previously (5). Polyclonal anti-ubiquitin antibody was obtained from Dako. Polyclonal anti-Tau Ser(P)[396] was obtained from Calbiochem. Monoclonal anti-α-tubulin and anti-HA clone HA-7 were obtained from Sigma. Lipofectamine was purchased from Invitrogen. Monoclonal

* This work was supported by grants-in-aid for scientific research on Priority Areas, Research on Pathomechanisms of Brain Disorders (to T. I. and M. H.) and Grant-in-aid for Scientific Research (C) 19590297 and 22500345 (to T. N.) from the Ministry of Education, Culture, Sports, Science, and Technology of Japan.

[S] The on-line version of this article (available at http://www.jbc.org) contains supplemental Figs. S1–S5.

[1] To whom correspondence may be addressed: Dept. of Molecular Neurobiology, Tokyo Institute of Psychiatry 2-1-8 Kamikitazawa, Setagaya-ku, Tokyo 156-8585, Japan. Tel.: 81-3-3304-5701; Fax: 81-3-3329-8035; E-mail: nonaka-tk@igakuken.or.jp.

[2] To whom correspondence may be addressed: Dept. of Molecular Neurobiology, Tokyo Institute of Psychiatry 2-1-8 Kamikitazawa, Setagaya-ku, Tokyo 156-8585, Japan. Tel.: 81-3-3304-5701; Fax: 81-3-3329-8035; E-mail: hasegawa-ms@igakuken.or.jp.

[3] The abbreviations used are: AD, Alzheimer disease; Aβ, amyloid β; PD, Parkinson disease; DLB, dementia with Lewy bodies; α-syn, α-synuclein; 3R1N, three-repeat Tau isoform with one amino-terminal insert; 4R1N, four-repeat Tau isoform with one amino-terminal insert; LA, Lipofectamine; LDH, lactate dehydrogenase.

anti-Tau T46 was from Zymed Laboratories Inc.. AT100 and HT7 antibodies were obtained from Innogenetics.

Preparation of α-Syn Seed, Oligomers, and Tau Fibrils—Human α-syn cDNA in bacterial expression plasmid pRK172 was used to produce recombinant protein (14). Wild-type (WT) or carboxyl-terminally HA-tagged α-syn was expressed in *Escherichia coli* BL21 (DE3) and purified as described (15). To obtain α-syn fibrils, α-syn (5–10 mg/ml) was incubated at 37 °C for 4 days with continuous shaking. The samples were diluted with 5 volumes of 30 mM Tris-HCl buffer (pH 7.5) and ultracentrifuged at 110,000 × *g* for 20 min at 25 °C. The pellets were resuspended in 30 mM Tris-HCl buffer (pH 7.5) and sonicated twice for 5 s each. The protein concentration was determined as described, and this preparation was used as Seed αS. In the case of α-syn oligomers, α-syn (10 mg/ml) was incubated at 37 °C for 3 days in the presence of 10 mM exifone. After incubation, the mixture was ultracentrifuged at 110,000 × *g* for 20 min at 25 °C. The supernatant was desalted by Sephadex G-25 (Amersham Biosciences) column chromatography, and eluted fractions (α-syn oligomers) were analyzed by reversed-phase HPLC, SDS-PAGE, and immunoblot analysis. Recombinant human three-repeat Tau isoform with one amino-terminal insert (3R1N) and four-repeat Tau isoform with one amino-terminal insert (4R1N) monomer and corresponding fibrils were prepared as described previously (16, 17).

Introduction of Proteins into Cells—Human neuroblastoma SH-SY5Y cells obtained from ATCC were cultured in DMEM/F-12 medium with 10% FCS. Cells at ~30–50% confluence in 6-well plates were treated with 200 μl of Opti-MEM containing 2 μg of the seed α-syn WT (Seed αS); HA-tagged α-syn (Seed-HA); α-syn monomers, oligomers; or Tau 3R1N or 4R1N fibrils; and 5 μl of Lipofectamine (LA) for 3 h at 37 °C. The medium was changed to DMEM/F-12, and culture was continued for 14 h. The cells were collected by treatment with 0.5 ml of 0.25% trypsin for 10 min at 37 °C, followed by centrifugation (1,800 × *g*, 5 min) and washing with PBS. The cellular proteins were extracted with 100 μl of homogenization buffer containing 50 mM Tris-HCl, pH 7.5, 0.15 M NaCl, 5 mM EDTA, and a mixture of protease inhibitors by sonication. After ultracentrifugation at 290,000 × *g* for 20 min at 4 °C, the supernatant was collected as a Tris-soluble fraction, and the protein concentration was determined by BCA assay. The pellet was solubilized in 100 μl of SDS-sample buffer. Both Tris-soluble and insoluble fractions were analyzed by immunoblotting with appropriate antibodies as indicated (15, 18).

Cell Culture Model of Seed-dependent Polymerization of α-Syn or Tau—α-Syn or Tau 3R1N or 4R1N was transiently overexpressed in SH-SY5Y cells by transfection of 1 μg of wild-type human α-syn cDNA in pcDNA3 (pcDNA3-α-syn) or human Tau cDNA in pcDNA3 (pcDNA3-Tau 3R1N or 4R1N) with 3 μl of FuGENE6 (Roche Applied Science) in 100 μl of Opti-MEM, followed by culture for 14 h. Under our experimental conditions, the efficiency of transfection with pEGFP-C1 vector was 20–30%. The cells were washed with PBS once, and then Seed αS, Seed-HA, Seed 3R1N, or Seed 4R1N was introduced with Lipofectamine as described above. The medium was changed to DMEM/F-12, and culture was continued for ~2–3 days. Cells were harvested in the presence of trypsin to digest extracellular cell-associated α-syn fibrils. The cellular proteins were differentially extracted and immunoblotted with the indicated antibodies, as described (18).

Confocal Microscopy—SH-SY5Y cells on coverslips were transfected with pcDNA3-α-syn and cultured for 14 h as described above, and then Seed αS was introduced, and culture was continued for ~1–2 days. After fixation with 4% paraformaldehyde, the cells were stained with appropriate primary and secondary antibodies as described previously (18). For thioflavin S staining, the cells were incubated with 0.05% thioflavin S at room temperature for 5 min. Fluorescence was analyzed with a laser-scanning confocal fluorescence microscope (LSM5Pascal, Carl Zeiss).

Immunoelectron Microscopy—For electron microscopy, cells overexpressing α-syn were transfected with Seed αS, cultured for 2 days, fixed in 0.1 M phosphate buffer containing 4% glutaraldehyde for 12 h, and then processed and embedded in LR White resin (London Resin, Reading, UK). Ultrathin sections were stained with uranyl acetate for investigation. Immunolabeling of the inclusions was performed by means of an immunogold-based postembedding procedure. Sections were blocked with 10% calf serum, incubated overnight on grids with anti-Ser(P)^{129} antibody at a dilution of 1:100, rinsed, then reacted with secondary antibody conjugated to 10-nm gold particles (E-Y Laboratories, San Mateo, CA) (1:10), rinsed again and stained with uranyl acetate.

Immunoelectron microscopic analysis of α-syn or Tau filaments extracted from cells was performed as follows. Cells overexpressing α-syn or Tau were transfected with Seed αS or Seed Tau, respectively. After incubation for 3 days, they were harvested, suspended in 200 μl of 10 mM Tris-HCl, pH 7.4, 1 mM EGTA, 10% sucrose, 0.8 M NaCl) and sonicated. The lysates were centrifuged at 20,400 × *g* for 20 min at 4 °C. The supernatant was recovered, and Sarkosyl was added (final 1%, v/v). The mixtures were incubated at room temperature for 30 min and then centrifuged at 113,000 × *g* for 20 min. The resulting pellets were suspended in 30 mM Tris-HCl, pH 7.5, placed on collodion-coated 300-mesh copper grids, and stained with the indicated antibodies and 2% (v/v) phosphotungstate. Micrographs were recorded on a JEOL 1200EX electron microscope.

Cell Death Assay—Cell death assay was performed using a CytoTox 96 non-radioactive cytotoxicity assay kit (Promega). TUNEL staining was performed using an *in situ* cell death detection kit (Roche Applied Science).

Assay of Proteasome Activity—SH-SY5Y cells transfected with pcDNA3-α-syn and Seed αS were cultured for 3 days or treated with 20 μM MG132 for 4 h. Cells were harvested, and cytosolic fraction was prepared as follows. Cells were resuspended in 100 μl of phosphate-buffered saline (PBS) and disrupted by sonication, and then insoluble material was removed by ultracentrifugation at 290,000 × *g* for 20 min at 4 °C. The supernatant was assayed for proteasome activity by using a fluorescent peptide substrate, benzyloxycarbonyl-Leu-Leu-Glu-7-amido-4-methylcoumarin (Peptide Institute, Inc.). 7-Amino-4-methylcoumarin release was measured fluorometrically (excitation at 365 nm; emission at 460 nm). In a green fluorescent protein (GFP) reporter assay of proteasome activity in living cells by confocal laser microscopy, SH-SY5Y cells trans-

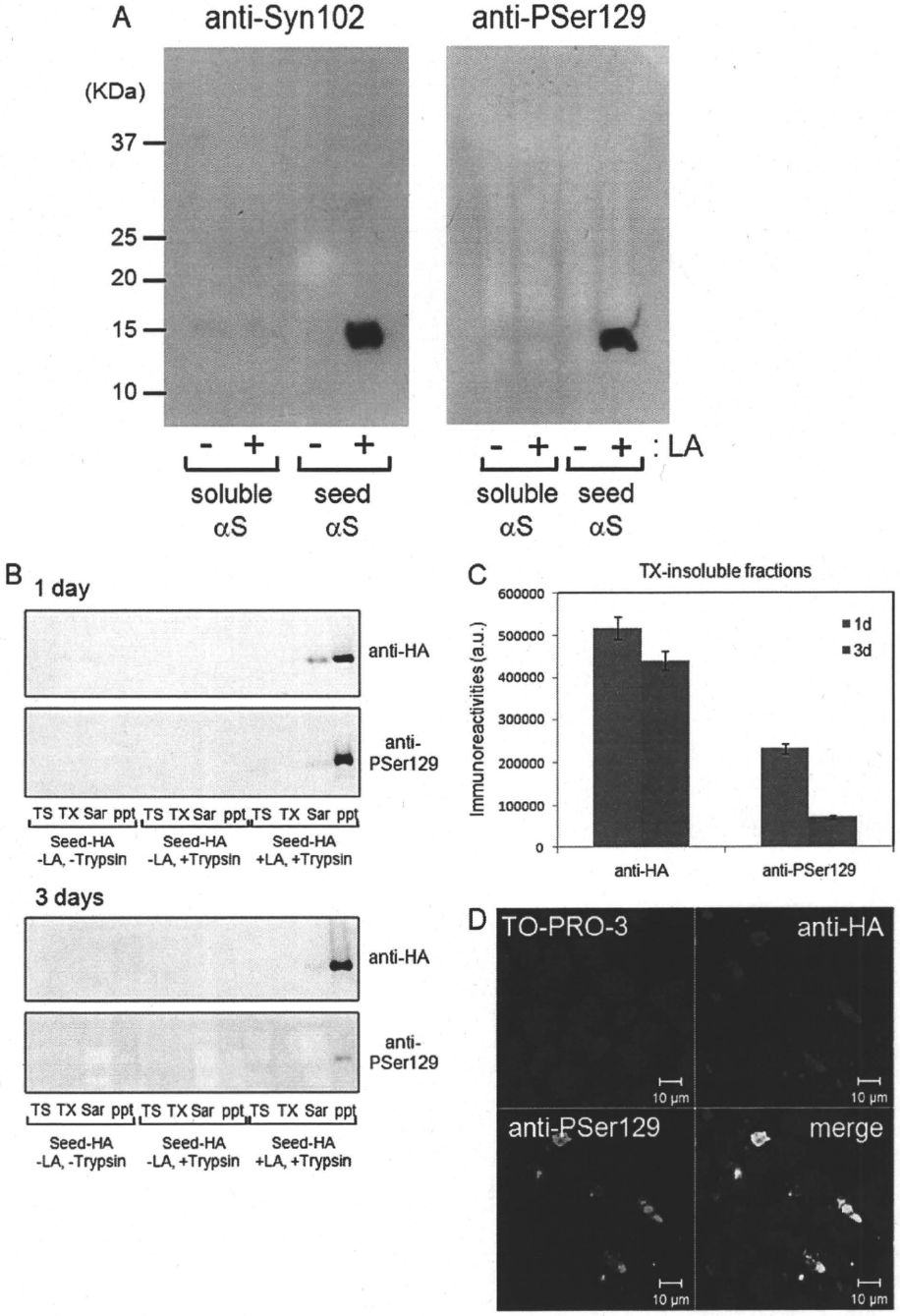

FIGURE 1. **Introduction of seed α-syn into cultured cells with Lipofectamine reagent.** *A*, purified recombinant α-syn (soluble form; 2 μg) and filaments (2 μg) were sonicated and then incubated with LA. The protein-LA complexes were dispersed in Opti-MEM and added to SH-SY5Y cells. After 14 h of culture, the cells were collected and sonicated in SDS sample buffer. After boiling, the samples were analyzed by immunoblotting with a phosphorylation-dependent anti-α-syn Ser(P)^{129} (*PSer129*) (*right*) or a phosphorylation-independent antibody, Syn102 (*left*). *B* and *C*, carboxyl-terminally HA-tagged α-syn fibril seeds (*Seed-HA*) were transduced into cells by the use of LA. After incubation for 1 day (*1d*) or 3 days (*3d*), cells were harvested with or without trypsin, and proteins were differentially extracted from the cells with Tris-HCl (*TS*), Triton X-100 (*TX*), and Sarkosyl (*Sar*), leaving the pellet (*ppt*). Immunoblot analyses of lysates using anti-HA and anti-Ser(P)^{129} are shown. The immunoreactive band positive for anti-HA or anti-Ser(P)^{129} in the Triton X-100-insoluble fraction was quantified. The results are expressed as means ± S.E. ($n = 3$). *D*, confocal laser microscopic analysis of cells treated with Seed-HA in the presence of LA. Cells were transduced with 2 μg of Seed-HA using 5 μl of LA. After a 48-h incubation, cells were fixed and immunostained with anti-Ser(P)^{129} (*green*) and anti-HA (*red*) and counterstained with TO-PRO-3 (*blue*).

fected with pcDNA3-α-syn (1 μg) and GFP-CL1 (0.3 μg) using FuGENE6 and then transfected with Seed αS were grown on coverslips for 2 days or treated with 20 μM MG132 for 6 h (19). These cells were analyzed using a laser-scanning confocal fluorescence microscope (LSM5Pascal, Carl Zeiss).

Statistical Analysis—The *p* values for the description of the statistical significance of differences were calculated by means of the unpaired, two-tailed Student's *t* test using GraphPad Prism 4 software (GraphPad Software).

RESULTS

Introduction of Seed α-Syn into Cultured Cells Using Lipofectamine Reagent—Cellular overexpression of α-syn by itself does not lead to fibrillization of α-syn in a form that resembles Lewy bodies. This prompted us to examine whether or not introduction of preformed aggregation seeds of α-syn (Seed αS) would elicit fibril formation. To introduce Seed αS into SH-SY5Y cells in a non-invasive manner, we tried several reagents used for transporting proteins or plasmid DNA into cells and found that LA, a cationic gene introducer, enables the introduction of Seed αS into SH-SY5Y cells. We were not able to detect any introduced α-syn monomer or fibrils following the simple addition of protein preparations to the culture medium, notwithstanding a previous report on this approach (20). The insoluble α-syn formed following LA-mediated Seed αS introduction was detected as buffer-insoluble α-syn in cell lysates (Fig. 1*A*). The insoluble α-syn was phosphorylated at Ser^{129} upon introduction into cells (Fig. 1*A*), indicating that Seed αS was incorporated in cells and phosphorylated intracellularly. Cells were harvested in the presence of trypsin to digest extracellular cell-associated α-syn fibrils. The optimal ratio of LA to Seed αS was about 5 μl to 2 μg of protein in 6-well plates. This treatment effectively introduced Seed αS not only into SH-SY5Y cells but also into several other types of cells examined, including Chinese hamster ovary cells and human embryonic kidney 293T cells (data not shown). In sharp contrast, soluble α-syn (either monomeric or oligomeric forms) was not introduced into the

cells by the same treatment (Figs. 1*A* and 4), suggesting that the LA treatment works exclusively for the internalization of insoluble α-syn aggregates.

These results strongly suggest that α-syn fibrils are incorporated with the aid of LA but do not exclude the possibility that extracellular α-syn fibrils may induce aggregation of endogenous α-syn without incorporation. To confirm that the extracellular α-syn fibril seeds are internalized into cells by LA, we performed the transduction of preformed carboxyl-terminally HA-tagged α-syn fibril seeds (Seed-HA) instead of non-tagged

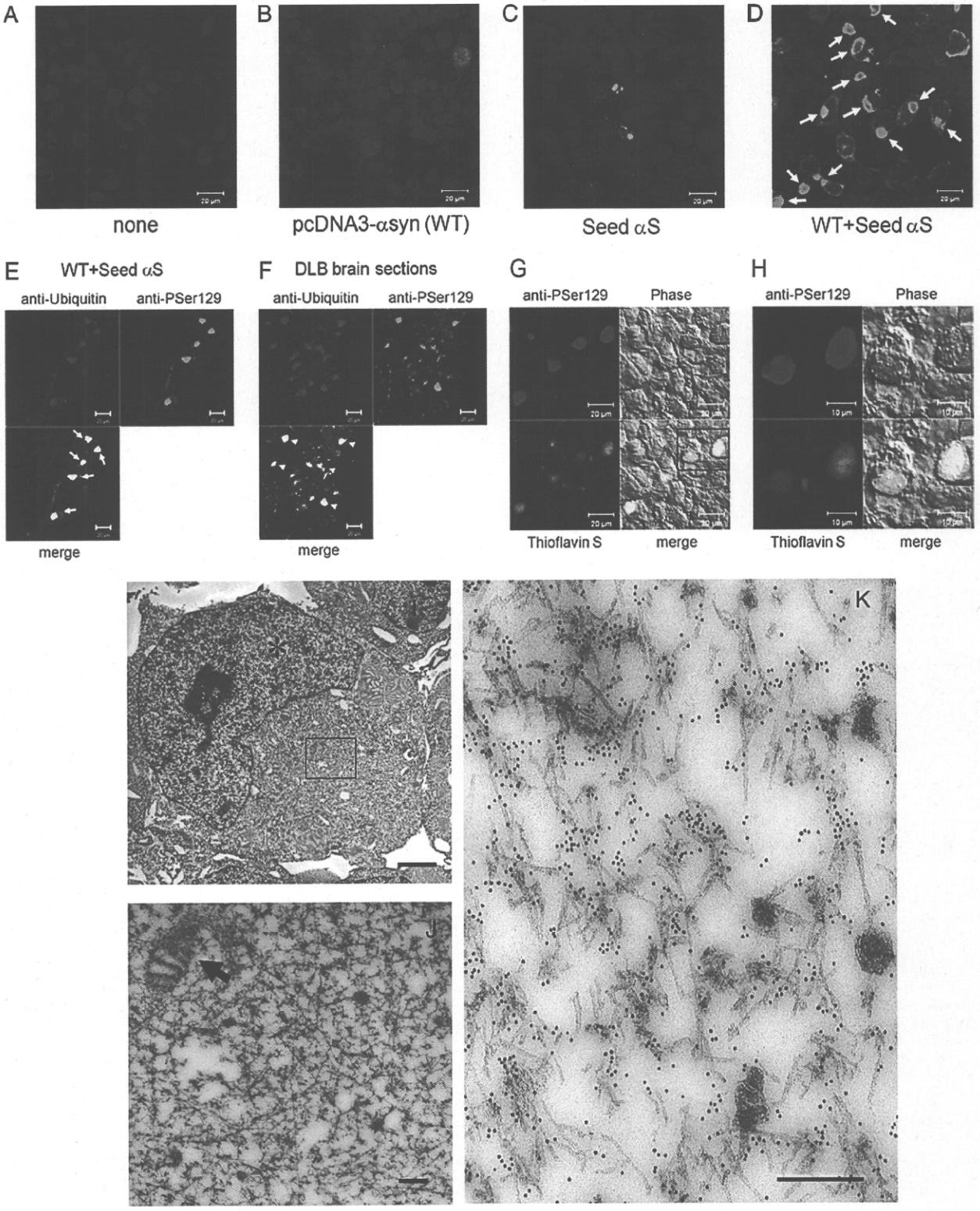

α-syn seeds. As shown in Fig. 1, *B* and *C*, time course experiments revealed that Seed-HA was also incorporated into cells in the presence of LA and could be detected with both anti-HA antibody and a phospho-α-syn-specific antibody (anti-Ser(P)^{129}), even 3 days after infection. Confocal microscopic analyses also indicated that Seed-HA was phosphorylated at Ser^{129} intracellularly. All anti-Ser(P)^{129}-positive dotlike structures were also stained with anti-HA, indicating that no endogenously phosphorylated α-syn aggregates are present in the cells (Fig. 1*D* and supplemental Fig. S1*C*).

Establishment of a Cell Culture Model for Nucleation-dependent Polymerization of α-Syn—Although introduction of the seed α-syn into cells was accompanied with phosphorylation, no further dramatic change was observed. Because the level of endogenous α-syn was relatively low in SH-SY5Y cells, we introduced non-tagged or HA-tagged seeds into cells transiently overexpressing α-syn. After 3 days of culture, immunocytochemistry for α-syn revealed a diffuse (Fig. 2*B*) or dotlike (Fig. 2*C*) pattern of cytoplasmic labeling by anti-Ser(P)^{129} in cells transfected with wild-type α-syn without seeds or in non-overexpressing cells with Seed αS, respectively. Surprisingly, however, in cells transfected with both pcDNA3-α-syn and Seed αS, we observed abundant round inclusions that occupied the cytoplasm and displaced the nucleus, with morphology highly reminiscent of cortical-type Lewy bodies observed in human brain (Fig. 2*D*). The size of the α-syn-positive inclusions was ~10 μm in diameter (Fig. 2*D*), which is similar to that of the Lewy bodies detected in the brains of patients with dementia with Lewy bodies. Similarly, when cells expressing α-syn were transfected with Seed-HA, abundant phosphorylated α-syn-positive cells were also detected (supplemental Fig. S1*D*).

We next examined the status of ubiquitin, which is positive in most types of intracellular filamentous inclusions, including Lewy bodies, in neurodegenerative disease brains. As shown in Fig. 2*E*, we found that almost all intracellular inclusions labeled with anti-Ser(P)^{129} were also positive for ubiquitin, as is the case for Lewy bodies in the cortex of human DLB brain (Fig. 2*F*). Furthermore, the juxtanuclear Ser(P)^{129}-positive, Lewy body-like inclusions were also positively labeled with thioflavin S, a fluorescent dye that specifically intercalates within structures rich in β-pleated sheet conformation (Fig. 2, *G* and *H*), indicating that the inclusions contain β-sheet-rich filamentous aggregates. Electron microscopic analysis of cells transfected with both wild-type α-syn and the seeds revealed that the inclusions are composed of filamentous structures ~10 nm in diameter that are often covered with granular materials (Fig. 2, *I* and *J*). The filamentous structures were randomly oriented within the cytoplasm of these cells, forming a meshwork-like profile, and were frequently intermingled with mitochondria (Fig. 2, *I* and *J*), being highly reminiscent of human cortical Lewy bodies. Immunoelectron microscopy showed that the filaments were densely decorated with anti-Ser(P)^{129} (Fig. 2*K*), demonstrating that they were composed of phosphorylated α-syn.

To biochemically validate this cellular model and to investigate further the molecular mechanisms underlying nucleation-dependent aggregation within cells, we differentially extracted α-syn from these cells using detergents of various strengths and analyzed the extracts by immunoblotting with anti-Syn102 and -Ser(P)^{129} antibodies. The levels of α-syn in the Sarkosyl-soluble and -insoluble fractions (total α-syn and α-syn phosphorylated at Ser^{129}, respectively) were dramatically increased in cells transfected with both wild-type α-syn and the seeds (*WT + Seed αS* in Fig. 3, *A* and *B*). To distinguish endogenous α-syn from exogenous α-syn fibrils, we used LA to transduce Seed-HA into cells overexpressing α-syn. Immunoblot analyses of these cells showed that HA-tagged α-syn with slower mobility than non-tagged α-syn was detected in the Sarkosyl-insoluble pellets as phosphorylated forms by anti-HA and anti-Ser(P)^{129} antibodies in cells treated with Seed-HA + LA (Fig. 3, *C–E*). Interestingly, in cells expressing α-syn (WT) treated with Seed-HA + LA, much more abundant non-tagged α-syn was detected in the Triton X-100- and Sarkosyl-insoluble fractions as phosphorylated forms with a smaller amount of the HA-α-syn. We also performed a dose dependence experiment with Seed-HA in cells expressing α-syn. As shown in supplemental Fig. S2, immunoreactive levels of Triton X-100-insoluble phosphorylated α-syn increased in parallel with an increase in the amount of Seed-HA. Furthermore, we tested whether Tau protein forms intracellular aggregates in the presence of α-syn seeds instead of Tau seeds. We found that Tau was not aggregated with Seed-HA, confirming that intracellular aggregate formation of soluble α-syn is specific to and dependent on fibril seeds of the same protein (supplemental Fig. S3). This nucleation-dependent polymerization of α-syn in cells was greater at 3 days than at 1 day after transduction of the seeds (Fig. 3*F*).

Negative stain electron microscopic observation of Sarkosyl-insoluble fractions of the cells harboring inclusions revealed anti-Syn102 and Ser(P)^{129}-positive filaments of ~5–10-nm width (Fig. 3, *G* and *H*) that are highly reminiscent of those derived from human α-synucleinopathy brains (21). Such filaments were never detected in the Sarkosyl-insoluble fraction of cells solely overexpressing α-syn (data not shown). These results indicated that the biochemical characteristics of α-syn accumulated in cells forming the Lewy body-like inclusions

FIGURE 2. **Confocal laser and electron microscopic analyses of α-syn inclusions in plasmid-derived α-syn-expressing cells treated with seed α-syn.** *A–D*, confocal laser microscopic analyses of control SH-SY5Y cells transfected with pcDNA3 vector and Lipofectamine alone (*A*), cells transfected with pcDNA3-α-syn (*WT*) (*B*), cells transduced with the seed α-syn (*Seed αS*) (*C*), and cells transfected with both pcDNA3-α-syn and Seed αS (*WT + Seed αS*) (*D*), immunostained with anti-Ser(P)^{129} (*green*), and counterstained with TO-PRO-3 (*blue*). The *arrows* indicate cytoplasmic round inclusions stained with anti-Ser(P)^{129} (*PSer129*). *Scale bars*, 20 μm. *E–F*, comparison of confocal images of cells transfected with both α-syn plasmid and Seed αS (*E*) and tissue sections from DLB brains (*F*) using anti-Ser(P)^{129} (*green*) and anti-ubiquitin antibodies (*red*). Cytoplasmic inclusions in transfected cells (*arrows*) are positive for ubiquitin, like Lewy bodies (*arrowheads*) in DLB brains. *Scale bars*, 20 μm. *G* and *H*, confocal microscopic images of cells transfected with both pcDNA3-α-syn and Seed αS. Cells were stained with 0.05% Thioflavin S (*green*) and anti-Ser(P)^{129} antibody (*red*). The *boxed area* on the *left* is shown in the *right panel*. *Scale bars*, 20 μm on the *left* and 10 μm on the *right*. *I* and *J*, electron microscopic analyses of cells transfected with both pcDNA3-α-syn and Seed αS. High magnification of the boxed area in *I* is shown in *J*. An *asterisk* or *arrow* indicates a nucleus or mitochondrion, respectively. *Scale bars*, 2 μm in *I* and 200 nm in *J*. *K*, immunoelectron microscopic observation of cells transfected with both pcDNA3-α-syn and Seed αS using a polyclonal antibody against phosphorylated Ser^{129} of α-syn. *Scale bar*, 200 nm.

were very similar to those of α-syn deposited in the brains of patients with α-synucleinopathies, including PD and DLB.

Because the idea has been gaining ground that transient oligomers, rather than mature fibrils, are responsible for cytotoxicity, we examined whether soluble oligomers could be introduced into cells in the same manner as fibril seeds by means of LA treatment and whether they could function as seeds for intracellular α-syn aggregate formation. As shown in Fig. 4, *A* and *B*, we purified stable α-syn oligomers from recombinant α-syn treated with exifone, an inhibitor of *in vitro* α-syn aggregation, which is thought to inhibit filament formation of α-syn by stabilizing SDS-resistant soluble oligomers (22, 23). Then cells expressing α-syn or mock plasmid were treated with a mixture of the oligomer fraction (5 μg) and LA and incubated for 3 days. Immunoblot analyses of lysates of these cells did not detect any SDS-resistant soluble oligomeric α-syn, and the levels of phosphorylated α-syn in the Sarkosyl-soluble and -insoluble fractions showed no increase (Fig. 4, *C* and *D*). On the other hand, we observed phosphorylated and deposited α-syn in the Sarkosyl-soluble and -insoluble fractions in cells expressing α-syn treated with Seed αS (Fig. 4, *C* and *D*). These results showed that SDS-resistant soluble oligomer of α-syn could not be introduced into cultured cells in the same manner as monomeric α-syn and/or could not function as seeds for intracellular α-syn aggregation.

Mutagenic Analysis of Nucleation-dependent Assembly of α-Syn—To investigate further the nucleation-dependent polymerization of α-syn, we analyzed the polymerization of α-syn mutated or truncated at various residues or subdomains that are believed to be crucial for its aggregation. Overexpression of A53T familial Parkinson mutant α-syn, which is readily fibrillogenic *in vitro*, in the presence of Seed αS moderately increased the accumulation and phosphorylation of α-syn in the Sarkosyl-soluble and insolu-

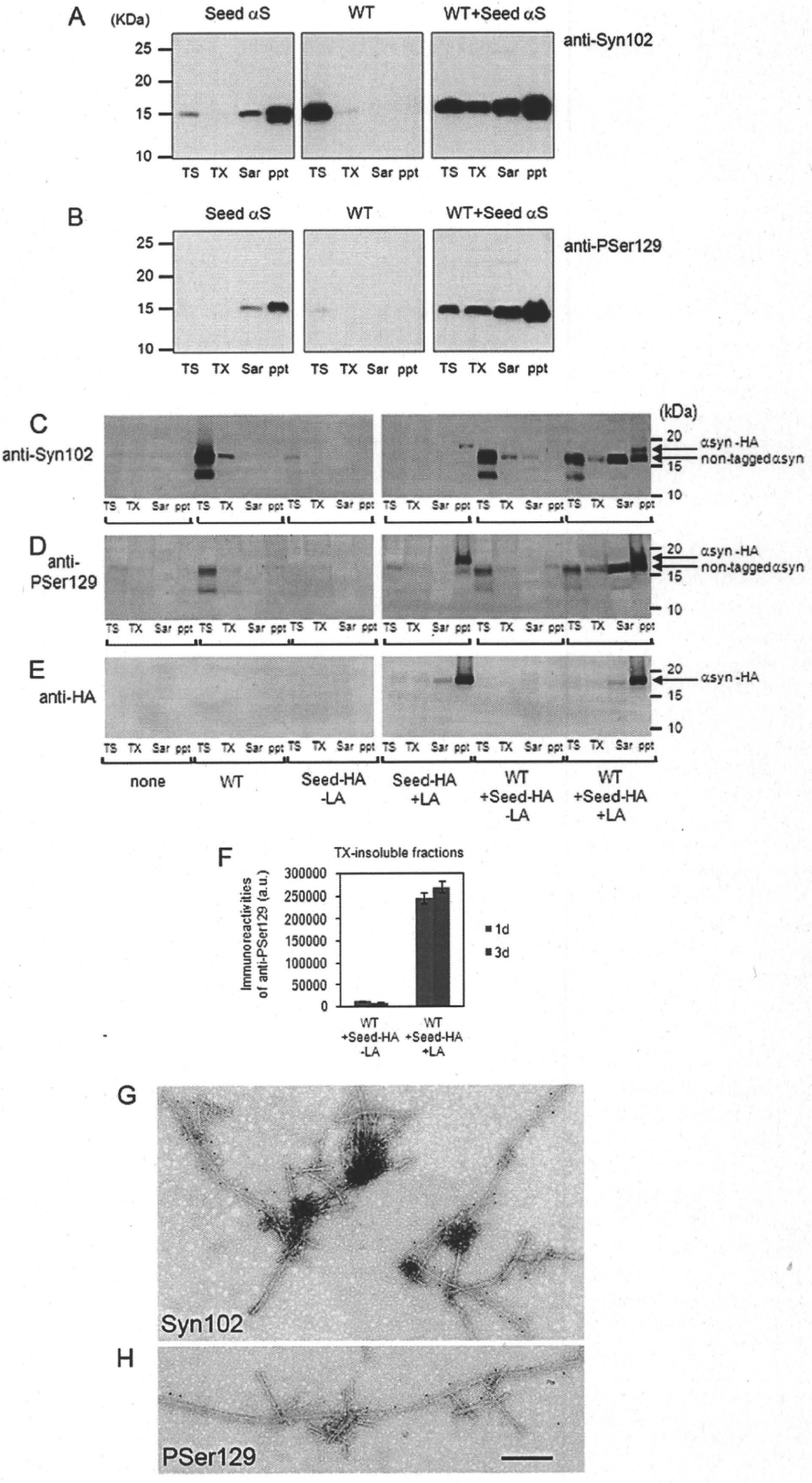

ble fractions compared with those in cells with wild-type α-syn expression and Seed αS (Fig. 5, *A* and *B*). In contrast, overexpression of Δ11 mutant α-syn, an assembly-incompetent mutant lacking residues 73–83, which have been shown to be essential for fibril formation of α-syn (24), elicited neither deposition nor phosphorylation of α-syn. We next introduced α-syn into SH-SY5Y cells expressing S129A mutant α-syn and observed slightly lower levels of Sarkosyl-insoluble α-syn compared with those in cells with wild-type α-syn expression and Seed αS. However, the frequency of inclusion bodies observed in seed-transduced cells expressing S129A was similar to that in seed-transfected cells expressing wild-type α-syn (data not shown), suggesting that phosphorylation at Ser^{129} is not required for the nucleation-dependent polymerization of α-syn within cells.

Nucleation-dependent Intracellular Polymerization of α-Syn Elicits Neurotoxicity and Cell Death—SH-SY5Y cells overexpressing α-syn started to show marked clumping suggestive of cellular degeneration and death by ~48 h after introduction of seeds (Fig. 6*B*). Quantitative analysis of cell death by a lactate dehydrogenase (LDH) release assay at 72 h after introduction of Seed αS showed that cells overexpressing wild-type, A30P, A53T, or S129A α-syn released ~30% of total LDH from total cell lysate, whereas only ~12% of LDH was released from cells expressing Δ11 mutant α-syn, which lacks polymerization ability. In control cells transfected with empty vector or pcDNA3-α-syn followed by treatment with Lipofectamine without seeds, only ~7% of LDH was released (Fig. 6*C*). These results suggest a close correlation between the seed-dependent aggregation of α-syn and cell death. However, the dying cells transfected with fibrillization-competent α-syn and seeds did not show typical morphological changes of apoptosis (*e.g.* nuclear fragmentation, positive TUNEL staining (supplemental Fig. S4*A*), or activation of caspase-3 (supplemental Fig. S4*B*)), suggesting that they did not undergo typical apoptotic cell death, despite a previous report that exposure to neuron-derived extracellular α-syn may cause apoptosis (25).

Impairment of Proteasome Activity in Cells with Intracellular Aggregates of α-Syn—Because α-syn is ubiquitinated in the brains of patients with α-synucleinopathies (26) and inhibition of ubiquitin-proteasome systems by aggregates of proteins with expanded polyglutamine tracts has been reported (27), we analyzed the ubiquitination state of cellular proteins in α-syn aggregate-forming cells and compared the pattern with that in cells treated with a proteasome inhibitor, MG132. A Sarkosyl-soluble fraction of seed-transduced cells expressing wild-type α-syn and harboring abundant inclusions showed increased levels of ubiquitin-positive staining, which was similar in pattern to that observed in cells treated with MG132 (Fig. 6*D*). Because this pattern suggested an impairment of the ubiquitin-proteasome system, we directly analyzed the proteasome activity of α-syn inclusion-forming cells using a specific fluorescent peptide substrate, benzyloxycarbonyl-Leu-Leu-Glu-7-amido-4-methylcoumarin, that emits fluorescence following proteasomal digestion and confirmed that proteasome activity was significantly reduced in these cells as well as in cells treated with 20 μM MG132 for 4 h (Fig. 6*E*). We further examined the suppression of proteasome activity using CL1, a short degron that has been reported to be an effective proteasome degradation signal (28) and whose fusion protein with green fluorescent protein (GFP-CL1) has been used as a reporter for inhibition of proteasomal activity by intracellular polyglutamine aggregates (27) and intracellular α-syn (19). To examine if intracellular α-syn inclusions affected proteasomal activity, SH-SY5Y cells were transfected with both wild-type α-syn and GFP-CL1, followed by the introduction of Seed αS. Fluorescent signals of GFP were scarcely detected in control cells transfected with GFP-CL1 alone (Fig. 6*F*, *none*) but were markedly increased upon treatment with proteasome inhibitor MG132 (Fig. 6*F*, *MG132*), confirming that GFP-CL1 was effectively degraded by proteasome. Strikingly elevated GFP signals were detected in cells forming α-syn inclusions (Fig. 6*F*, *WT + Seed αS*) compared with those in control cells (Fig. 6*F*, *none* or *WT*), and GFP-CL1 and deposits of phosphorylated α-syn were co-localized within these cells (*arrowheads*). These results strongly suggest that proteasome activity is impaired in cells harboring α-syn inclusions elicited by the introduction of Seed αS.

Small Molecular Inhibitors of Amyloid Filament Formation Protect against Cell Death Induced by Seed-dependent α-Syn Polymerization—We have previously shown that several classes of small molecular compounds inhibit amyloid filament formation of α-syn, Tau, and Aβ *in vitro* (17, 23). These observations prompted us to test whether these inhibitors exert a protective effect against death of SH-SY5Y cells mediated by the nucleation-dependent polymerization of α-syn. Fig. 7*A* shows the effects of three polyphenol compounds, exifone, gossypetin, and quercetin, and a rifamycin compound, rifampicin, added to the culture media at a final concentration of 20 or 60 μM. Remarkably, all of these compounds blocked cell death, with gossypetin being the most effective. Our previous *in vitro* studies elucidated that several polyphenols, including gossypetin and exifone, inhibit α-syn assembly and that SDS-stable, noncytotoxic soluble α-syn oligomers are formed in their presence (23), suggesting that such polyphenols may inhibit filament formation of α-syn by stabilizing soluble, prefibrillar intermediates. Gossypetin or exifone might suppress intracellular α-syn aggregate formation by stabilizing such soluble intermediates in cultured cells as well. Immunoblot analysis

FIGURE 3. **Immunoblot and immunoelectron microscopic analyses of intracellular α-syn aggregates in cultured cells.** *A* and *B*, immunoblot analysis of α-syn in cells treated with Seed αS alone (*Seed αS*), pcDNA3-α-syn alone (*WT*), or both WT and Seed αS (*WT + Seed αS*). Proteins were differentially extracted from the cells with Tris-HCl (*TS*), Triton X-100 (*TX*), and Sarkosyl (*Sar*), leaving the pellet (*ppt*). Blots were probed using anti-α-syn (Syn102) (*A*) and anti-$Ser(P)^{129}$ (*PSer129*) (*B*). *C–F*, immunoblot analysis of proteins differentially extracted from mock (none) or cells transfected with pcDNA3-α-syn (*WT*), cells transduced with Seed-HA with (*Seed-HA + LA*) or without LA treatment (*Seed-HA − LA*), and cells overexpressing α-syn treated with Seed-HA with (*WT + Seed-HA + LA*) or without LA treatment (*WT + Seed-HA − LA*). Immunoreactivity of phosphorylated α-syn in the Triton X-100-insoluble fraction was quantified using anti-$Ser(P)^{129}$, and the results are expressed as means ± S.E. ($n = 3$), as shown in *F*. a.u., arbitrary unit. *G* and *H*, immunoelectron microscopy of α-syn filaments extracted from transfected cells. SH-SY5Y cells were transfected with both pcDNA3-α-syn and Seed αS. Sarkosyl-insoluble fraction was prepared from the cells, and the filaments were immunolabeled with anti-Syn102 (*G*) or $Ser(P)^{129}$ (*H*) antibody. *Scale bar*, 200 nm. *1d* and *3d*, 1 and 3 days, respectively.